

DESIGN OF A COMPLIANT MECHANISM TO AMPLIFY THE STROKE OF
A PIEZOELECTRIC STACK ACTUATOR

A THESIS SUBMITTED TO
THE GRADUATE SCHOOL OF NATURAL AND APPLIED SCIENCES
OF
MIDDLE EAST TECHNICAL UNIVERSITY

BY

TAMER KESKİN

IN PARTIAL FULLFILLMENT OF THE REQUIREMENTS
FOR
THE DEGREE OF MASTER OF SCIENCE
IN
MECHANICAL ENGINEERING

FEBRUARY 2013

Approval of the thesis:

**DESIGN OF A COMPLIANT MECHANISM TO AMPLIFY THE STROKE
OF A PIEZOELECTRIC STACK ACTUATOR**

submitted by **TAMER KESKİN** in partial fulfillment of the requirements for the degree of **Master of Science in Mechanical Engineering Department, Middle East Technical University** by,

Prof. Dr. Canan Özgen
Dean, Graduate School of **Natural and Applied Sciences** _____

Prof. Dr. Suha Oral
Head of Department, **Mechanical Engineering, METU** _____

Assist. Prof. Dr. Gökhan O. Özgen
Supervisor, **Mechanical Engineering Dept., METU** _____

Examining Committee Members:

Prof. Dr. Kemal Özgören
Mechanical Engineering Dept., METU _____

Assist. Prof. Dr. Gökhan O. Özgen
Mechanical Engineering Dept., METU _____

Assist. Prof. Dr. Ergin Tönük
Mechanical Engineering Dept., METU _____

Assist. Prof. Dr. Ender Ciğeroğlu
Mechanical Engineering Dept., METU _____

Dr. Ümit Ceyhan
TUBİTAK SAGE _____

Date: **01.02.2013**

I hereby declare that all information in this document has been obtained and presented in accordance with academic rules and ethical conduct. I also declare that, as required by these rules and conduct, I have fully cited and referenced all material and results that are not original to this work.

Name, Last name: Tamer KESKİN
Signature:

ABSTRACT

DESIGN OF A COMPLIANT MECHANISM TO AMPLIFY THE STROKE OF A PIEZOELECTRIC STACK ACTUATOR

KESKİN, Tamer
M. Sc., Department of Mechanical Engineering
Supervisor: Assist. Prof. Dr. Gökhan O. Özgen

February 2013, 59 pages

Main objective of this study is to design a compliant mechanism with high frequency and high mechanical amplification ratio to be used for amplifying the stroke of a piezostack actuator. In this thesis, first of all, related literature is investigated and then alternative conceptual designs are established utilizing the mechanisms found in literature survey. Once best conceptual design is selected, detailed design of this mechanism is done. For detailed design of the compliant mechanism, topology optimization method is used in this study. To design the mechanism, first a design domain is defined and then a finite element model of the design domain is prepared to be used in topology optimization runs. After running the topology optimization model by using TOSCA with ANSYS, results are imported to ANSYS, where final performance of the mechanism design is checked. After finalizing design of the mechanism, it is produced and its performance is tested through experiments.

Keywords: Compliant mechanism, mechanism design, mechanical amplification, topology optimization, piezostack actuator

ÖZ

BİR PIEZOELEKTRİK STACK EYLEYİCİNİN ÇIKIŞ DEPLASMANINI ARTTIRMAK İÇİN KULLANILACAK BİR ESNEK MEKANİZMANIN TASARIMI

KESKİN, Tamer
Yüksek Lisans, Makina Mühendisliği Bölümü
Tez Yöneticisi: Yar.Doç. Dr. Gökhan Özgen

Şubat, 2013, 59 sayfa

Bu çalışmanın temel amacı, bir piezostack eyleyicinin çıkış deplasmanını arttırmak için kullanılabilir yüksek frekanslı ve yüksek büyütme oranlı bir esnek mekanizma tasarlamaktır. Bu tez çalışmasında öncelikle ilgili alanyazın araştırılmış ve daha sonra alanyazın araştırmasında yer alan esnek mekanizmalar temel alınarak alternatif kavramsal tasarımlar oluşturulmuştur. Bu alternatif tasarımlardan bir tanesi seçildikten sonra bu tasarımın detaylandırılması çalışmalarına başlanılmıştır. Esnek mekanizmanın detay tasarım çalışmasında topoloji optimizasyonu tekniği kullanılmıştır. Mekanizmayı tasarlamak için önce tasarım alanı tanımlanmış ve daha sonra topoloji optimizasyonu için sonlu elemanlar modelleri hazırlanmıştır. TOSCA'yı ANSYS ile birlikte kullanarak topoloji optimizasyonu gerçekleştirildikten sonra, sonuçlar ANSYS'e aktarılarak mekanizma tasarımı son haline getirilmiştir. ANSYS ortamında mekanizma tasarımının son halinin performansı kontrol edildikten sonra, mekanizmanın bir prototipi üretilmiş ve bu prototip üzerinde performans deneyleri gerçekleştirilmiştir.

Anahtar Kelimeler: esnek mekanizma, mekanizma tasarımı, mekanik yükseltme, topoloji optimizasyonu, piezostack eyleyici

To my family

ACKNOWLEDGEMENTS

I would like to express my sincere gratitude to my advisor, Assist. Prof. Dr. Gökhan O.Özgen for his guidance, support and suggestions throughout the study.

I would also like to express my sincere appreciation for my lovely wife Esra for her valuable friendship, support and help.

For their understanding my spending lots of time on this work, my sincere thanks go to my sister and to my mother.

I am also grateful to my company ASELSAN and my coworkers Bayram, Serap Hakan and Gökhan for their encouragement and support during my thesis.

Lastly, for his great support for my education throughout his life I am also grateful to my father in heaven.

TABLE OF CONTENTS

ABSTRACT.....	vi
ÖZ.....	vii
ACKNOWLEDGEMENTS.....	ix
TABLE OF CONTENTS.....	x
LIST OF TABLES.....	xi
LIST OF FIGURES.....	xii
CHAPTERS	
1.INTRODUCTION.....	1
2.LITERATURE SURVEY.....	3
2.1 Literature Survey of Articles.....	3
2.2 Literature Survey of Commercial Products.....	5
2.3 Literature Survey of Books.....	5
2.4 Categorization of Compliant Mechanisms.....	5
2.5 Types of Compliant Mechanism.....	13
3.CONCEPTUAL DESIGN.....	15
3.1 Introduction.....	15
3.2 Presented Conceptual Designs.....	15
3.2.1 Concept 1: Simple Lever 1.....	15
3.2.2 Concept 2: Simple Lever 2.....	16
3.2.3 Concept 3: Double Lever 1.....	16
3.2.4 Concept 4: Double Lever 2.....	17
3.3 Evaluation of concepts.....	18
4.DETAILED DESIGN.....	21
4.1 Topology Optimization Method as a Tool to Design Distributed Compliant Mechanism.....	21
4.2 Design Iterations.....	23
4.2.1 First Design Iteration.....	24
4.2.2 Second Design Iteration.....	30
4.2.3 Third Design Iteration.....	43
4.2.4 Detailed Analysis of the Selected Compliant Mechanism.....	47
5.MANUFACTURING AND TESTING OF THE COMPLIANT MECHANISM..	49
6.CONCLUSION.....	57
REFERENCES.....	59

LIST OF TABLES

TABLES

Table 1 First set of properties of compliant mechanisms for mechanical amplification found in the literature	7
Table 2 Second set of properties of compliant mechanisms for mechanical amplification found in the literature	9
Table 3 Weight of evaluation criterion	19
Table 4 Points of concepts from the criterion	19
Table 5 Input and output displacements of the final design of the compliant mechanism for linear and nonlinear analysis options (no resistive spring is connected to the output node).....	47
Table 6 Static measurement results of the compliant mechanism: Comparison of experimental and analysis results.....	54
Table 7 Static displacement analysis results when orthotropic material model is used	54
Table 8 Dynamic measurement results of the compliant mechanism	56

LIST OF FIGURES

FIGURES

Figure 1 Simple Lever Concept 1	16
Figure 2 Simple Lever Concept 2	16
Figure 3 Double Lever Concept 1	17
Figure 4 Double Lever Concept 2.....	18
Figure 5 Conceptual Design	23
Figure 6 Half symmetry of conceptual design.....	23
Figure 7 1.st lever of conceptual design.....	24
Figure 8 2nd lever of conceptual design.....	24
Figure 9 Design domain for the first lever section of the compliant mechanism.....	25
Figure 10 Displacement response for the final configuration of the topology optimization run (first lever section part of the compliant mechanism)	25
Figure 11 Static displacement analysis of the first lever section of the compliant mechanism by ANSYS (design obtained from topology optimization results) .	26
Figure 12 Conceptual design of the 2 nd lever	27
Figure 13 Finite element model of the design domain to be used in the topology optimization of the 2.nd lever (added lever is for increasing the lateral stiffness of the mechanism)	27
Figure 14 Result of the topology optimization for the 2 nd lever (density factor distribution of all elements)	28
Figure 15 Static displacement analysis results for the final design of the 2 nd lever	28
Figure 16 Finite element model of the compliant mechanism which is a combination of 1 st and 2 nd lever designs.....	29
Figure 17 Static displacement analysis results of analysis done for the final design of the compliant mechanism	29
Figure 18 Finite element model of the design domain to be used in the topology optimization of the double lever mechanism: Second design iteration.....	31
Figure 19 Result of topology optimization (density factor distribution) of the double lever design domain for a resistive spring constant of $k=3\text{N/mm}$ and volume reduction constraint of %40	32
Figure 20 Output node y-displacement given as a function of iterations performed during the topology optimization run: for a resistive spring constant of $k=3\text{N/mm}$ and volume reduction constraint of %40	33
Figure 21 Result of topology optimization (density factor distribution) of the double lever design domain for a resistive spring constant of $k=3\text{N/mm}$ and volume reduction constraint of %60	33
Figure 22 Output node y-displacement given as a function of iterations performed during the topology optimization run: for a resistive spring constant of $k=3\text{N/mm}$ and volume reduction constraint of %60	33
Figure 23 Result of topology optimization (density factor distribution) of the double lever design domain for a resistive spring constant of $k=3\text{N/mm}$ and volume reduction constraint of %80	34

Figure 24 Output node y-displacement given as a function of iterations performed during the topology optimization run: for a resistive spring constant of $k=3\text{N/mm}$ and volume reduction constraint of %80	34
Figure 25 Result of topology optimization (density factor distribution) of the double lever design domain for a resistive spring constant of $k=1\text{N/mm}$ and volume reduction constraint of %40	35
Figure 26 Output node y-displacement given as a function of iterations performed during the topology optimization run: for a resistive spring constant of $k=1\text{N/mm}$ and volume reduction constraint of %40	36
Figure 27 Result of topology optimization (density factor distribution) of the double lever design domain for a resistive spring constant of $k=1\text{N/mm}$ and volume reduction constraint of %60	36
Figure 28 Output node y-displacement given as a function of iterations performed during the topology optimization run: for a resistive spring constant of $k=1\text{N/mm}$ and volume reduction constraint of %60	37
Figure 29 Result of topology optimization (density factor distribution) of the double lever design domain for a resistive spring constant of $k=1\text{N/mm}$ and volume reduction constraint of %80	37
Figure 30 Output node y-displacement given as a function of iterations performed during the topology optimization run: for a resistive spring constant of $k=1\text{N/mm}$ and volume reduction constraint of %80	38
Figure 31 Final geometry of the double lever design obtained using the results of topology optimization (density factor distribution) of the original domain for a resistive spring constant of $k=3\text{N/mm}$ and volume reduction constraint of %60	39
Figure 32 Displacement result of the second optimization, final design of the double lever mechanism without any resistance spring (Second design iteration)	39
Figure 33 Displacement result of the final design of the double lever mechanism without any resistance spring (Second design iteration)	40
Figure 34 Thin areas of the final design of the double lever mechanism without any resistance spring (Second design iteration)	40
Figure 35 Displacement results of the modified final design (with thickened sections) of the double lever mechanism without any resistance spring (Second design iteration)	41
Figure 36 Full geometry of the modified final design (with thickened sections) of the double lever mechanism without any resistance spring (Second design iteration)	41
Figure 37 Full geometry of the second modified final design (with stiffening hinge removed) of the double lever mechanism without any resistance spring (Second design iteration): High amplification ratio version	42
Figure 38 Displacement results of the second modified final design (with stiffening hinge removed) of the double lever mechanism without any resistance spring (Second design iteration): High amplification ratio version	42
Figure 39 Finite element model of the design domain to be used in the topology optimization of the double lever mechanism: Third design iteration	44
Figure 40 Result of topology optimization (density factor distribution) of the double lever design domain for a resistive spring constant of $k=0.2\text{N/mm}$ and volume reduction constraint of %70	44

Figure 41 Output node y-displacement given as a function of iterations performed during the topology optimization run: for a resistive spring constant of $k=0.2\text{N/mm}$ and volume reduction constraint of %70.....	45
Figure 42 Result of topology optimization (density factor distribution) of the double lever design domain for a resistive spring constant of $k=0.2\text{N/mm}$ and volume reduction constraint of %80	45
Figure 43 Output node y-displacement given as a function of iterations performed during the topology optimization run: for a resistive spring constant of $k=0.2\text{N/mm}$ and volume reduction constraint of %80.....	46
Figure 44 Stress results for selected compliant mechanism.....	48
Figure 45 Prototype compliant mechanism manufactured using fast prototyping using ULTEM 9085 as fast prototyping material	50
Figure 46 Piezostack actuator amplification system with base plate and sensors	50
Figure 47 Setup for measuring static and dynamic performance of the prototype compliant mechanism	51
Figure 48 High voltage amplifier and display unit for laser displacement sensors	52
Figure 49 Oscilloscope.....	52
Figure 50 Function Generator	53
Figure 51 Dynamic signal analyzer	53
Figure 52 Frequency response function result on dynamic signal analyzer	55
Figure 53 Frequency response function analysis result for different modulus of elasticity	55

CHAPTER 1

INTRODUCTION

Design of a compliant mechanism which can amplify the stroke of a piezostack actuator is the main focus of this thesis work. Piezostack actuators can produce high forces (up to 1000 N). They have resonance frequencies mostly more than 1000Hz, which is important for high frequency applications. Typical maximum stroke of piezostack actuators is about %0.1 of their length, i.e. maximum displacement of a 100mm piezostack actuator would be about 0.1mm. In order to increase the stroke of a piezostack actuator compliant mechanisms are frequently used.

A compliant mechanism is defined in the literature as a mechanism without joints. For this type of mechanisms, degrees of freedom (DOF) needed for the mechanism is provided by the flexibility of the links that form the mechanism. With the help of flexure hinges (instead of joints) with small input displacements, high output displacements can be attained. Output displacement over input displacement which may be called the mechanical amplification ratio, is a parameter desired to be high as much as possible when the mechanism is designed to be used with a piezostack actuator.

In this thesis, a compliant mechanism to be used to amplify the 90 μ m stroke of a particular piezostack actuator as much as possible. In order to design such a compliant mechanism to provide a high mechanical amplification of the stroke of a linear actuator, topology optimization is used, as explained in the literature survey presented in Chapter 2. After the investigation of the literature in the field of compliant mechanisms given in Chapter 2, conceptual designs are presented in Chapter 3. In Chapter 3, conceptual designs are also evaluated according to the evaluation criterion given in the same chapter. Detailed analyses of the selected design alternative for the compliant mechanism are performed in Chapter 4. Topology optimization method is used to design of the compliant mechanism. Using TOSCA and ANSYS, finite element models used in optimization runs are constructed. In various design iterations, results obtained from TOSCA is remodeled and analyzed in ANSYS again to check the final performance of the compliant mechanism designed using topology optimization results. Results of optimization runs and performance of various design iterations are presented in Chapter 4. Production and testing of the final design of the compliant mechanism is explained in Chapter 5. Concluding remarks are presented in Chapter 6.

CHAPTER 2

LITERATURE SURVEY

In this chapter literature survey is investigated from articles, commercial products and books. Compliant mechanisms which are designed to amplify the mechanical displacement output of linear actuators in articles give more information about their design parameters and output features. Commercial products gives mostly more intuition to designers how they are used. They also gives information about their about force and displacements. The literature survey for books is a little bit different than previous two literature survey types. They mostly represent type of compliant mechanisms, which equations can be used to design them and etc. In the following sections, three type of literature survey will be investigated detailed. During this literatures survey, amplification ratio (AR) is defined as output displacement divided by input displacement

2.1 Literature Survey of Articles

In the study of K.B. Choi *et al.* [1], a compliant mechanism is analyzed with respect to some parameters. In this article the general structure of the mechanism is shown, which is named as “Mechanism 1” to be used in one of the following sections where a categorization of compliant mechanism designs is made. There are 4 fixed points on the mechanism. The input for this mechanism is given from two piezostack actuators. Input and output directions are perpendicular to each other. Leaf flexure hinges are used due to their high amplification ratio. The optimization analysis of the mechanism is done according to the parameters of the leaf flexure, which are the lateral distance between centerlines of upper and lower hinges, length of hinge and the thickness of the hinge.

The amplification mechanism presented in this paper has a stroke of 400 μ m with a lowest natural frequency of 40 HZ and resolution of 50nm is demonstrated. Moreover the amplification ratio (ratio of output displacement response to input displacement) of the mechanism is found as 13.

R.F. Osborn *et al.* [2] designed a distributed compliant mechanism using topology optimization. This type of compliant mechanism is one of the best mechanisms for a high stroke and high frequency compliant mechanism. This mechanism is named as “Mechanism 2” to be revisited in later sections of this thesis. It has an amplification ratio of 20 and has a nominal operating frequency of 90 Hz. However the mechanism has a limit of 240 Hz operating frequency. The mechanism is fixed from 7 points. This type of fixing may be due to increase of high frequency also. In this mechanism a voice coil motors is used as the actuator. Input and the output are in the same direction for this mechanism. The input for the mechanism is 0.25 mm and the output is 5 mm.

In the study of M. Frecker *et al.* [3], design of a compliant mechanism using topology optimization is explained. To design a compliant mechanism first a design area is constructed, then the inputs are given and finally after iterations the desired mechanism topology is derived. However the amplification ratio of this example is less than the aim of the thesis study. In this mechanism a piezostack actuator is used as an actuator. This mechanism is named as “Mechanism 3” and will be revisited in later sections of this thesis.

In the study of H.W. Ma *et al.* [4], the design of a compliant mechanism using analytical models are investigated. The method used here is very similar to the method presented in this literature survey as the first paper. The joints are expressed as a torsion and axial

spring in order to model the amplification ratio. This mechanism is named as “Mechanism 4” and will be revisited in later sections of this thesis..

According to the study of D.C. Handley *et al.* [5], the design of the compliant mechanism is done using flexure hinges instead of revolute joints. , the compliant mechanism is modeled like a four bar however there are no revolute joints. The representation of the compliant mechanism is valid for small angular displacements. The mechanism is named as “Mechanism 5” and will be revisited in later sections of this thesis.

S. Kota *et al.* [6] explained the methodology of a topology design for a compliant mechanism in their study. The design procedure in this paper is as follows: a) required kinematic motion, b) required stiffness to an external load, c) design space, d) material properties, e) stress limitations, f) buckling instabilities, g) dynamic considerations and h) weight limitations. The main objective function for the design of the compliant mechanism is maximizing geometrical advantage and minimizing total strain energy. Topology optimization is used to design the mechanism with desired amplification performance. This mechanism is named as “Mechanism 6a”.In the same paper, another mechanism is also represented which has a first natural frequency of 3884 Hz and mechanical advantage of 12 (maximum output of the mechanism is 20 μ m).. This mechanism is called as “Mechanism 6b” and will be revisited in later sections of this thesis.

In the study of L. Ren *et al.* [7], the design of a compliant mechanism for MEMS application is done using topology optimization. The mechanism which is designed is a gripper mechanism. First the design domain of the mechanism is created and then the analysis done with stress and volume constraint. The mechanisms designed in this paper are named as “Mechanism 7a” and “Mechanism 7b”. After this optimization two material compliant mechanism analyses is done with volume and stress constraint of the materials.

In the study of G.W. Jang *et al.* [8], first the design of 3 compliant mechanisms for MEMS application is done using topology optimization and then using shape optimization stress and displacement values are optimized. In this method, first the topology optimization is applied to a design domain and then the shape optimization is applied. According to the needs, the stress and displacement values are optimized with shape optimization. The performance increase with shape optimization by the first mechanism is %80, which is named as “Mechanism 8a”. The output displacements before and after shape optimization are 1.9 μ m and 3.4 μ m respectively. In another design shown, first the design domain and objective is defined as in the “Mechanism 8a” and then first topology and then shape optimization is done. After shape optimization the output performance of the mechanism is increased %300, which is defined as “Mechanism 8b”. The output displacements before and after shape optimization are 0.65 μ m and 2.56 μ m respectively. A third mechanism designed in the same paper, which is called “Mechanism 8c”, has a perpendicular amplification direction according to the input direction. The same procedure is also applied to this mechanism as the previous 2 mechanisms. The output displacements before and after shape optimization are 0.74 μ m and 2.26 μ m respectively. After shape optimization, the output performance of the mechanism is increased %200.

In the study of S. Kota *et al.* [9], first of all, some compliant mechanisms with different outputs for MEMS applications are introduced. One of them is actuated with Shaped Memory Alloy (SMA) wire. The mechanism is named as “Mechanism 9”.

As the other topology problems, in the study of S.C. Huang *et al.* [10], first the design domain is defined and the design domain of the mechanism is 5mmx4mm and the thickness of the mechanism is 0.5mm. This mechanism can also be classified as an inverter mechanism because the output displacement direction is parallel but in the negative direction of the input direction. After the analysis is done the output displacement is 23 μ m. The mechanism is named as “mechanism 10”Topology optimization is used for the design of this mechanism.

2.2 Literature Survey of Commercial Products

The piezoelectric stage XY 25XS by CEDRAT company [11] is based on standard Amplified Piezo Actuator (APA®) and owns high stiffness. The compliant mechanism used to amplify the input of the piezostack actuator named as “Mechanism 11”.

The Double Tip Tilt mechanism DTT35XS-space by CEDRAT company [11] is named as “Mechanism 12. It is a very light piezoelectric mechanism (25 grams). The mechanism uses Strain Gauges as positioning sensor and allows to reach a 1:4000 stability (1 μ rad rms) The mechanism is ideal for pointing mechanisms or laser beam steering.

The mechanism of the parallel pre-stressed actuator PPA10M by CEDRAT company [11] is named as “Mechanism 13”. IA typical application for this product is laser Cavity tuning in LIDAR and other opto-electronic functions.

The mechanism of the amplified piezoelectric actuator APA120ML by CEDRAT company [11] is called as “Mechanism 14”. This product is designed to obtain a stiff actuator and produce higher displacements compared to direct piezoelectric actuators.

The mechanism of the hollow parallel pre-stressed actuator (HPPA) by CEDRAT company [11] is named as “Mechanism 15”. This product is a direct piezo actuator with an 8mm diameter internal hole available for an optical function.

2.3 Literature Survey of Books

In the literature survey of books, many mechanisms are found which can be helpful for conceptual design. The mechanisms found in this survey cannot be categorized with other mechanisms in literatures survey because there are almost no features presented for these mechanisms in the books. One of the biggest favors of these books to present us is lever type mechanisms.

Levers can be used in compliant mechanisms to achieve a high gain amplification ratio [12]. Many alternative conceptual designs for lever type compliant mechanisms for amplifying piezostack actuator strokes are available in [12] and [13].

2.4 Categorization of Compliant Mechanisms

In this section compliant mechanisms presented in previous sections are categorized with respect to their features. A total of 22 mechanisms and their features are tabulated in Table 1 and Table 2. For each table, information on same mechanisms are given but with respect to different features. These tables will be very helpful for choosing conceptual designs for this thesis study because it will enable us to compare all features of compliant mechanisms for mechanical amplification available in the literature.

Among the features used to categorize the mechanisms investigated, first one (column 2 of Table) is important. It is on the type of optimization method used in design of the mechanism. Most of the mechanisms which are analyzed in literature survey are designed using structural optimization methods. These methods can be categorized into two groups: Parameter Optimization, Topology Optimization. When parameter optimization approach is used in the design of a compliant mechanism, parameters of the flexure hinges are optimized according to the natural frequency and amplification ratio of the mechanism. Thickness of the flexure hinge, lateral distance between centers of the upper and lower hinges, and length of the flexure hinge are some of the parameters which are optimized. When topology optimization approach is used in the design of a compliant mechanism, material distribution in a chosen design domain is optimized for an objective function defined in terms of input-output relationship desired for the mechanism to be designed. This optimization approach is commonly adopted for the design of distributed compliant mechanisms. Finally, shape optimization approach is also commonly used to complement other optimization approaches used in the design of a compliant mechanism for decreasing stress concentration values of flexure hinges or flexible links.

Table 1 First set of properties of compliant mechanisms for mechanical amplification found in the literature

Mechanism No	Type of optimization method used in design of the mechanism	2D or 3D	Directional relationship Between Output and Input	First Natural Frequency in Hz	Amplification Ratio	Type of Actuation Used	Type of Material Used to Construct the Mechanism
1	Parametric optimization according to the hinge dimensions is used	2D	Perpendicular Relationship	40	13	Piezostack actuator is used as actuation.	Aluminum
2	Topology and Shape optimization is used for the design	2D	Parallel collinear Relationship	240	20	Piezostack actuator and voice coil motor is used as actuation.	No information, but seems like plastic according to the picture
3	Topology and Shape optimization is used for the design	2D	Parallel collinear Relationship		3.2	Piezostack actuator is used as actuation.	Aluminum
4	Parametric optimization according to the hinge dimensions is used	2D	Perpendicular Relationship	201	Graph is given	Piezostack actuator is used as actuation.	No information
5	Position analysis is done , no optimization is made for this design	2D	Angular Relationship	No information	No information	No information	No information
6(a)	Topology and Shape optimization is used for the design	2D	Perpendicular Relationship	No information	No information	MEMS actuator	No information, but seems plastic according to the picture
6(b)	Topology and Shape optimization is used for the design	2D	Parallel collinear Relationship	3884	12 in static application, 20 in dynamic application	MEMS actuator, electrostatic comb-drive actuator is used as actuator.	No information, but seems plastic according to the picture
7(a)	Topology optimization is done	2D	Perpendicular Relationship	No information	1.97	MEMS actuator	E=180 GPa
7(b)	Topology optimization is done for the design	2D	Perpendicular Relationship	No information	2.105	MEMS actuator	E1=180 GPa and E2=60 GPa, two material in a compliant mechanism is used

Table 1 (Continued)

8(a)		Topology and Shape optimization is used for the design	2D	Parallel collinear Relationship but in the negative direction	No information	No information	MEMS actuator	$E=1.7 \times 10^5 \mu\text{N}/(\mu\text{m})^2$
8(b)		Topology and Shape optimization is used for the design	2D	Parallel Relationship with lateral offset but in the negative direction	No information	No information	MEMS actuator	$E=1.7 \times 10^5 \mu\text{N}/(\mu\text{m})^2$
8(c)		Topology optimization is done	2D	Perpendicular Relationship	No information	No information	MEMS actuator	$E=1.7 \times 10^5 \mu\text{N}/(\mu\text{m})^2$
9		Topology optimization is done for the design	2D	Perpendicular Relationship	No information	No information	SMA is used as actuator	No information but seems plastic
10		Topology optimization is used for the design	2D	Parallel collinear Relationship	No information	No information	Piezostack is used as actuator	The modulus of elasticity of the material is 4.4 GPa
11	No		3D	Output and input has almost any kind of relationship.	2200Hz	No information	Piezostack actuator	No information
12	No		3D	Output and input has almost any kind of relationship.	3200Hz	No information	Piezostack actuator	No information
13	No		2D	Output and Input has collinear parallel linear relationship.	65000Hz	No information	Piezostack actuator	No information
14	No information		2D	Perpendicular Relationship	6450	No information	Piezostack Actuator	No information
15	No information		2D	Linear Relationship	20000Hz	No information	Piezostack Actuator	No information

Table 2 Second set of properties of compliant mechanisms for mechanical amplification found in the literature

Mechanism No	Effective Temperature Range	Input Force and Input Displacement Ranges	Output Force and Displacement Range	Type of Control for Actuator	Actuator Dimension	Mechanism Dimensions	Target Mode of Use(Static or Dynamic Response)
1	No information	0-38 μm input displacement	0-488 μm output displacement	Open loop	10mmx36mm x10mm	54mmx56mm x36mm	Designed for static applications, however can be used also in dynamic application
2	No information	0-250 μm input displacement	0-5mm output displacement	No information	No information	No information	Designed for dynamic application
3	No information	Not given, must be 0-20 μm according to the piezoconcept of %0.1 length increase	Not given but must 0-64 μm output displacement according to the gain amplification.	No information	7mmx7mmx20mm	5.5 in. x 3 in.x0.25in	No information but indicates that piezostack actuator are used for dynamic applications rather then quasi static applications.
4	No information	No information	No information	No information	No information	40mmx20mm x0.4mm	Designed for static application
5	No information	1.2 Nm and 0.97°	No information	No information	No information	50mmx60mm	No information
6(a)	No information	No information	No information	No information	No information	No information	No information
6(b)	No information	No information	0-20 μm output displacement	No information	No information	No information	Designed for dynamic application
7(a)	No information	0-2.86 μm input displacement and 1 N input force	No information about force however it can be derived by stiffness of the spring attached to the output port and gain amplification	No information	No information	800 μm x800 μm x7 μm	No information

Table 2 (Continued)

7(b)	No information	0-2.86µm input displacement and 1 N input force	No information about force however it can be derived by stiffness of the spring attached to the output port and gain amplification	No information	No information	800µmx800µm x7µm	No information
8(a)	No information	The input force is 5N	The output displacement is 3.435 µm and the output force can be derived from the stiffness of the spring	No information	No information	800µmx800µm x6µm	No information
8(b)	No information	The input force is 5N	The output displacement is 2.563 µm and the output force can be derived from the stiffness of the spring	No information	No information	800µmx800µm x6µm	No information
8(c)	No information	The input force is 5N	The output displacement is 2.260 µm and the output force can be derived from the stiffness of the spring	No information	No information	800µmx800µm x6µm	No information
9	No information	The input force range is 14.47 N	No information	No information	No information	No information	Not defined but when using SMA it should be for static application.
10	No information	The input force of the actuator is 6 N and the input displacement is 22.32 µm	The output force of the actuator is 0.7 N and the output displacement is 28 µm	No information	No information	4000µm x 5000µm x 500µm	Not defined
11	No information	No information	In XY plane 20µm and out of Z plane 0.5µm. Max rotation about Z axis is 50µrad and according to X and Y axis 10µrad	Closed Loop	No information	50mmx50mmx 18mm	Designed for dynamic application

Table 2 (Continued)

12	-20/75°C	No information	Max Displacement 35µm in XY plane and out of Z plane 10µm. Max angular displacement is 2µm	Closed Loop	No information	Diameter 30mm asnd height is 22mm	Designed for dynamic application
13	No information	No information	Max Displacement 8µm and maximum force is 800N	Closed Loop	No information	9mmx9mmx28mm	Designed for static application
14	-20 / 75 °C	No information	Max Displacement 130µm and maximum force is 1400N	Closed Loop	No information	22.5mmx78.9mmx45mm	Designed For Dynamic Application.
15	-40 / 65 °C	No information	Max Displacement 22µm	Closed Loop	No information	Diameter 30mm Height 37mm	Designed For Static Application.

2.5 Types of Compliant Mechanism

Compliant mechanisms are classified according to their type of flexure. Compliant mechanisms which have elastic deformation just near flexural or notch hinges are called lumped compliant mechanisms [14]. Compliant mechanisms which have fully compliance are called “Distributed compliant mechanisms”. For example, cantilever beams can be called distributed compliant mechanisms, because they have fully compliance when forces act on it [14].

CHAPTER 3

CONCEPTUAL DESIGN

3.1 Introduction

In the first part of this thesis work, various alternative conceptual designs are created utilizing the design alternatives found in the literature survey. After defining these concepts, they are going to be evaluated considering the performance needs of the amplification mechanism to be designed. In this chapter, first proposed alternative mechanism designs are presented and then evaluation criteria are defined. Afterwards, best concept is chosen according to evaluation results.

3.2 Presented Conceptual Designs

In this part, four different mechanisms are developed from mechanisms found in literature survey. Main design idea that all conceptual designs proposed is based on is the lever concept.

3.2.1 Concept 1: Simple Lever 1

In this concept, as seen clearly from Figure 1, mechanical advantage of lever mechanism is used. Displacement applied from point A is amplified at point B because center of rotation of the lever is point F. However, there is no joint at point F. Area around point F up to the lever could be considered as the flexure hinge. This flexure hinge should be designed considering the target amplification ratio, stress concentration and fatigue failure conditions.

Amplification ratio of this mechanism is equal to $\frac{(b+a)}{a}$ when there is a rotary joint at F

and when the length of the hinge above F is 0. If the ratio b/a is increased, amplification ratio will be increased however the force applied from point A should be increased according to the output force needed at point B. In this concept the input and output are in the same direction.

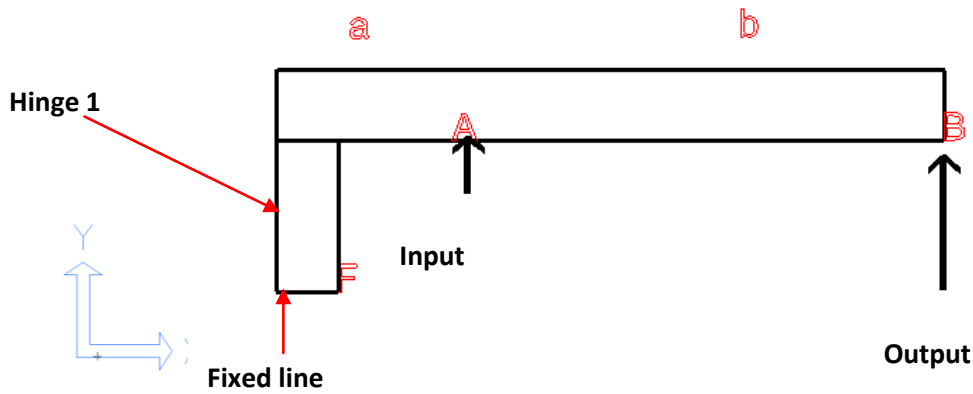


Figure 1 Simple Lever Concept 1

3.2.2 Concept 2: Simple Lever 2

This concept is very similar to concept 2 except the fact that there is one little change in the relationship between the direction of the input and output (Figure 2). They are parallel but in negative directions. This concept also needs a hinge design like concept 2.

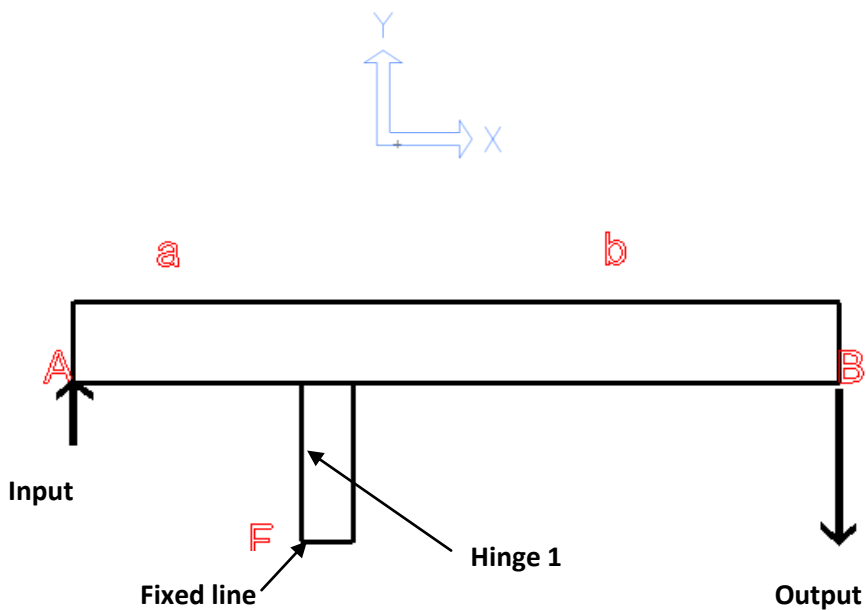


Figure 2 Simple Lever Concept 2

3.2.3 Concept 3: Double Lever 1

This concept (see Figure 3) is a double lever concept which is formed by combining two levers so that the amplification ratio. First amplification is done between points B and A and the second one is done between points C and B. There are two fixing points (F and F*) of this mechanism. Effective amplification ratio of the first lever step depends on the first hinge and projection of the link lengths b and a on x axis. Second amplification ratio

also depends on the hinge around F^* and on projections of link lengths b^* and c on the x axis. It is like joining two simple levers.

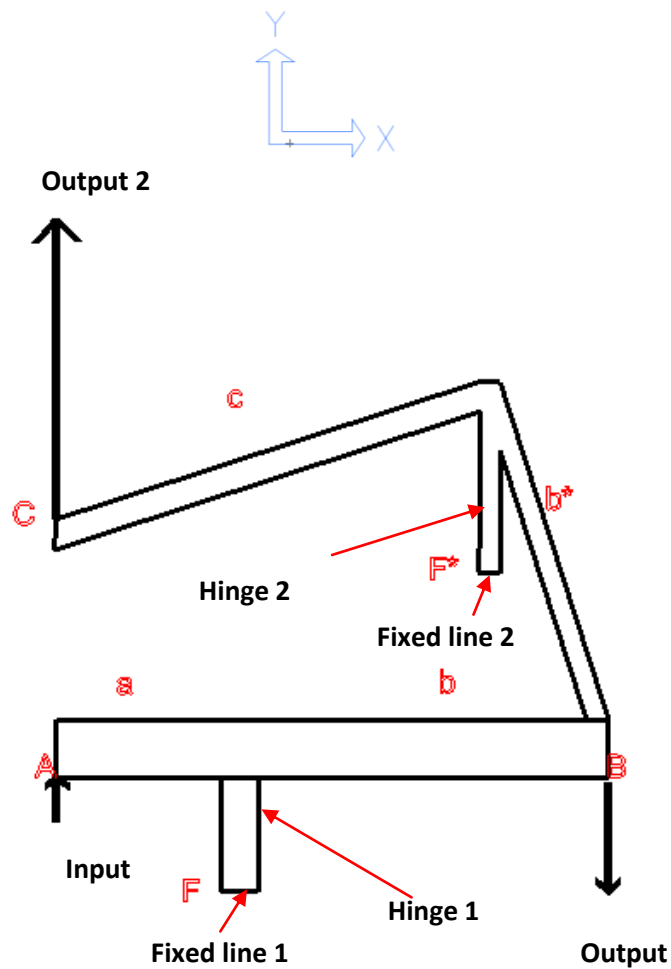


Figure 3 Double Lever Concept 1

3.2.4 Concept 4: Double Lever 2

This concept (see Figure 4) is very similar to concept 3. In this concept, two levers are joined to increase mechanical amplification. Joined lever mechanisms are taken from concept 1 and concept 2. In this concept, hinge area around point F should be optimized. Difference between concept 4 and 3 is the relative directions of input and output. Direction of output is in the opposite direction.

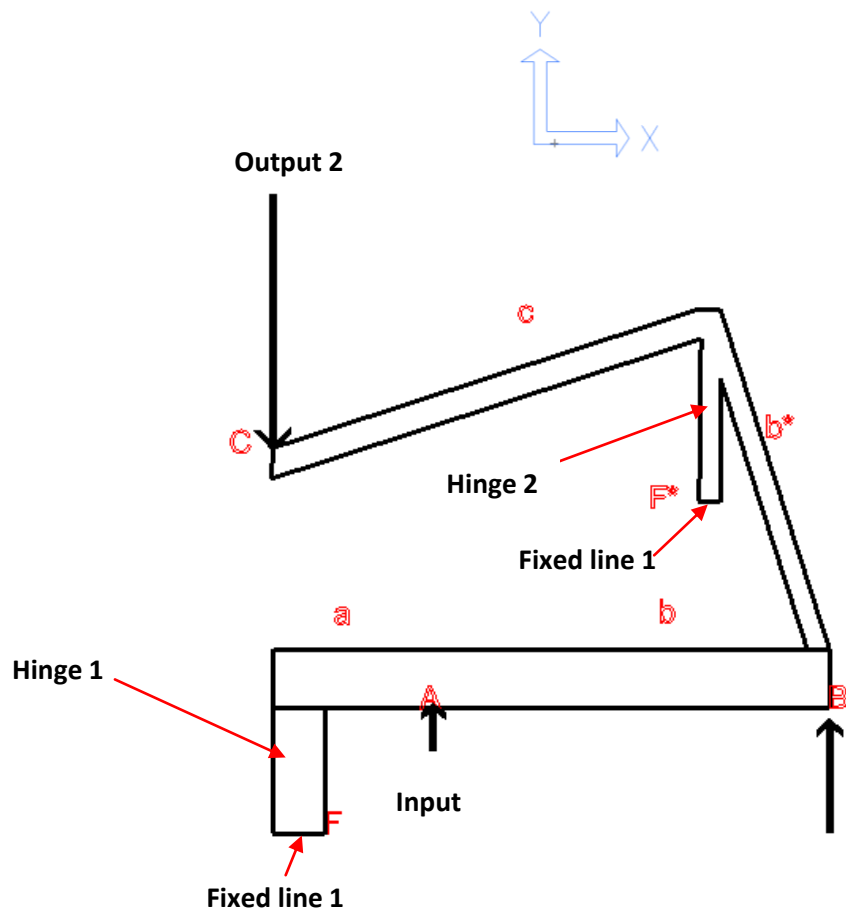


Figure 4 Double Lever Concept 2

3.3 Evaluation of concepts

In this section, presented concepts in previous section are evaluated in terms of their amplification ratio, first natural frequency, ease of implementation, dimensions, input-output relationships and cost. After this evaluation the best concept will be chosen according to their points collected from the evaluation.

In this section, weights of the criterion are defined in Table 3. . As seen clearly from Table 3, for our purpose high amplification ratio and high first natural frequency is the most important features and that's why they have the highest weight in evaluation. Concepts will have points for each criterion from 1 to 10 and then these points will be multiplied with the weight of criterion. Results of the evaluation are given in Table 4. So according to the evaluation results, concept 3 is chosen in this thesis. Concept 3 and 4 has the highest points from the amplification ratio feature. Actually many of their features have the same points however due to more simple application in terms symmetry concept 3 is chosen to be designed in detail, which will be explained in the following chapter.

Table 3 Weight of evaluation criterion

Criterion	Weight
Amplification Ratio	4
Frequency(First Natural Frequency)	2.5
Simplicity	1.5
Dimension	1
Input output direction relationship	0.7
Cost	0.3
Total	10

Table 4 Points of concepts from the criterion

Criterion	1	2	3	4
Amplification Ratio	5	5	10	10
Frequency	7	7	5	5
Simplicity	7	7	4	2
Dimension	8	8	5	5
Input output direction relationship	8	5	10	6
Cost	8	8	5	5
Total	64	61.9	72	66.2

CHAPTER 4

DETAILED DESIGN

In designing compliant mechanism there are many ways. It can be designed using analytical expressions which do not give always good results and also they cannot be used in all geometry types. Due to that reason, in this thesis, design of a high stroke and high frequency compliant mechanism will be done using topology optimization. As seen from the literature, topology optimization is used mostly by design of distributed compliant mechanisms. In this work, topology optimization will be used both for distributed and lumped compliant mechanisms. In this thesis, a piezostack actuator will be used as an actuator and this type of actuators have very limited displacement ranges (between 20 μ m and 200 μ m). Due to that reason in the design of a compliant mechanism high amplification ratio is very important.

4.1 Topology Optimization Method as a Tool to Design Distributed Compliant Mechanism

Topology optimization is the most difficult optimization process in structural optimization [14]. By topology optimization the aim is to find the optimum material distribution in a defined design domain. The known parameters in a topology optimization are design domain, material properties, objective function, boundary conditions, design restrictions and volume constraints (amount of volume reduction) [16]. Topology optimization is used mostly for decreasing the volume or mass of structure by preserving the stiffness of the structure as much as possible. It may also be used to maximize the natural frequencies of a structure using the least amount of material.

In topology optimization, design domain should be modeled first. It should be considered that a certain portion of the design domain will give us the desired compliant mechanism. As mentioned, topology optimization is mostly used for the design of stiff structures, however in this thesis it will be used to design of a distributed compliant mechanism. In topology optimization, an initial design domain is modeled using finite elements. Each

element is assigned a density factor ρ_i using which the effective modulus of the material is calculated as

$$E_i = E_o \rho_i \quad \text{Equation 1 [14]}$$

Where E_o is actual young modulus. Element mass density is also calculated as the product of density factor and the actual density of the material used to define the particular finite element. In topology optimization the density factor for each finite element becomes one of the optimization parameters while objective function is defined in terms of responses at chosen DOFs of the model. Constraints are usually defined in terms of the reduction in the total mass of the design domain which is calculated using the mass density values multiplied with the density factor. At each iteration of the optimization, density factors are updated so that both the objective is achieved and mass constraints are satisfied. In order to end up with a physically realizable material distribution, density factor of each element is either changed towards a value of unity or towards a value of zero. A density factor close to zero means that the particular element can be removed from the design domain.

Topology optimization for designing distributed compliant mechanisms is implemented by defining a design domain which is defining the spatial boundaries of the final mechanism. In order to converge to a specific geometry for the compliant mechanism within the space occupied by the design domain, a certain mass (or volume reduction) constraint is specified. Depending on the functional needs of the mechanism to be designed, loads and the responses of interest are identified and objective function is defined in terms of the responses of DOFs of interest. Using the resulting the material distribution (in terms of density factors of each element), a specific geometry for the compliant mechanism is extracted and detail design of the mechanism is based on that extracted geometry.

In this work, TOSCA will be used to implement the topology optimization method to design the compliant mechanism. TOSCA is a subprogram which works with many solvers like ANSYS or ABACUS. Design domain is first created and meshed in ANSYS Classic. Afterwards the .cdb file is created to give an input to TOSCA. Finally, the objective function constraints frozen elements are defined in TOSCA and optimization is running. In this section topology optimizations will be done using a design domain meshed with plane strain elements and element size of 0.4mm. Plane strain elements are used because all strains are assumed to be on xy plane. All of the topology optimizations which are done in this chapter are done according to the static structural case. The ideal case would also include maximizing the

4.2 Design Iterations

Actually the desired generic geometry of the final design of the compliant mechanism is illustrated in Figure 5. But in order to decrease the topology optimization time, symmetry of the mechanism will be utilized and the design work will be done on one half of the mechanism shown in Figure 6.

A total of three iterations are performed in the detail design phase until a final detail design for the mechanism is reached. First one includes design of two levers separately using topology optimization and combining the resulting level designs in series to increase the overall amplification of the mechanism. In the second iteration, two levers are designed simultaneously. Generic geometry defined in Figure 5 is used to define a design space and topology optimization in TOSCA environment is used to maximize output for a given input with for various volume reduction constraints. In the third iteration, the design domain is defined such that the resulting material distribution would form flexural hinges and the resulting compliant mechanism would be of lumped compliant mechanism type.

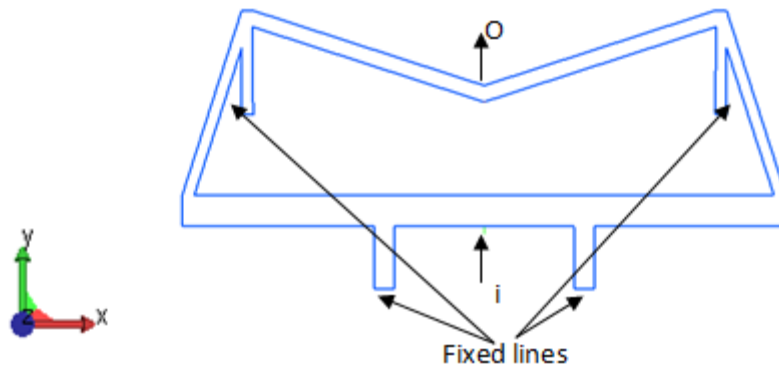


Figure 5 Conceptual Design

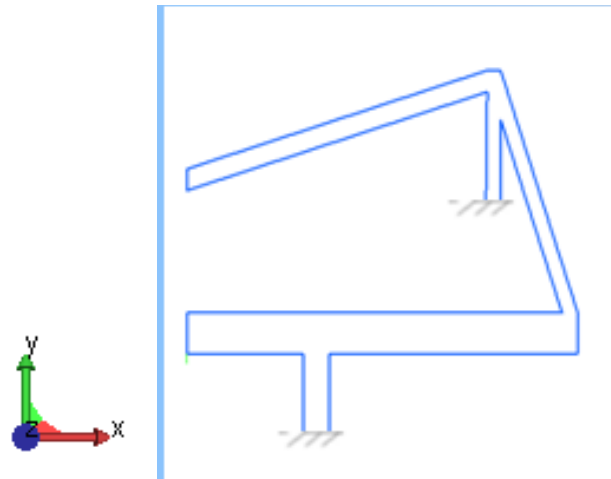


Figure 6 Half symmetry of conceptual design

4.2.1 First Design Iteration

When this mechanism is analyzed it can be seen that it is a combination of two levers, 1st lever and 2nd lever (see Figure 7 and Figure 12). In the first design iteration, these are designed separately and combined at the end. Overall amplification ratio of the combined mechanisms is evaluated. Aluminum is chosen as the material to construct the mechanism.

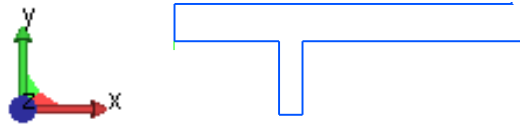


Figure 7 1.st lever of conceptual design

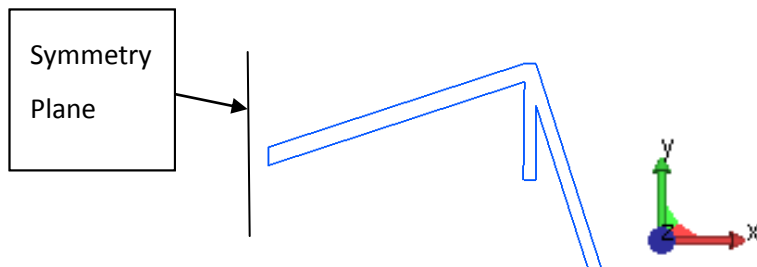


Figure 8 2nd lever of conceptual design

As seen in the Figure 9, for the 1st lever an almost triangular design domain is defined first. Red elements are chosen as frozen elements to prevent them from being eliminated in the optimization. Other blue elements constitute the design domain. In this first iteration aluminum is chosen as material and the thickness of the material is 2 mm. As the loading condition, a displacement of 50 μ m (sample piezostack actuator displacement) is given in y direction at the input node (see Figure 9). Objective of the topology optimization run is defined as maximizing the displacement at the output node in negative y direction. As volume constraint, decreasing volume of the design domain to %60 is chosen. Material distribution obtained after topology optimization is given in Figure 66. For this material distributions, y-direction displacement at the output node turned out to be 400 μ m in the – y direction. Resulting amplification ratio for the first lever is 8:1.

After the optimization stage, next step is converting the material distribution obtained from topology optimization results into a physical design. This will be done by creating a CAD file from the material distribution. This is a tedious and manual process since TOSCA only gives out the mesh that is the result of the topology optimization (elements with non-zero density factor are present in that mesh), so it should be converted manually in a CAD program. This work is done in I-DEAS environment. After converting the mesh into a drawing, it is remeshed and analyzed in ANSYS environment. Resulting output displacement is 340 μ m (see Figure 11). As seen clearly the result is not the same as it is given from TOSCA. This is due to the fact that mesh used to form the final geometry included some elements with density factors smaller than one but in the final model these elements will have to be used with unity density factor. As a result, the final mechanism is expected to be stiffer compared to the mechanism that came out of the topology optimization run. Next, second lever is designed using a similar procedure.

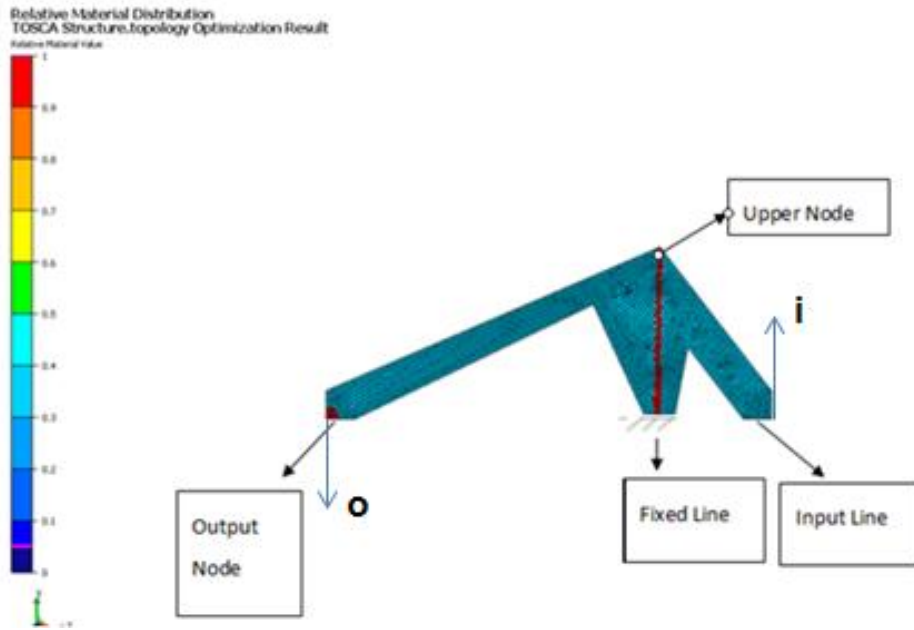


Figure 9 Design domain for the first lever section of the compliant mechanism



Figure 10 Displacement response for the final configuration of the topology optimization run (first lever section part of the compliant mechanism)

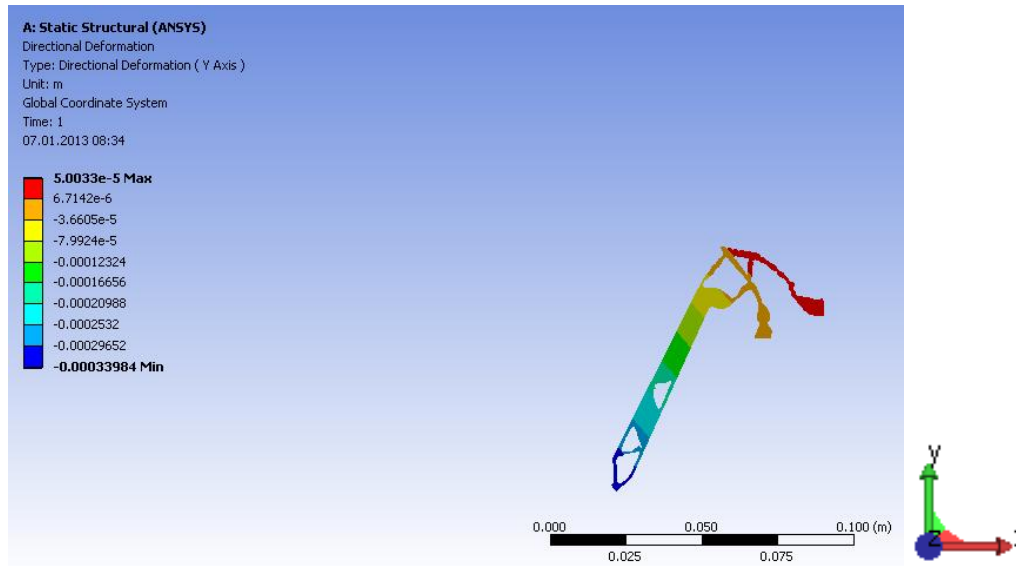


Figure 11 Static displacement analysis of the first lever section of the compliant mechanism by ANSYS (design obtained from topology optimization results)

Conceptual design of the second lever is given Figure 12. A modification is made to this design As illustrated in Figure 13 a second hinge area is added to the design domain with the purpose of increasing the stiffness of the lever structure in the lateral direction thus increasing the lowest natural frequency. Final design domain for the second lever is given in Figure 13. In the design domain, red elements are the frozen elements (not part of the optimization) to prevent them from being eliminated during the optimization and these elements are chosen mostly as boundary condition elements or nodes. Elements that are blue constitute the design domain. Another important criterion is resisting force at the output location. Since mechanism to be designed based on topology optimization results will be used as a mechanical amplification system for a low stroke piezostack actuator, there will be a load at the output of the mechanism. This resistive load will also have to be included in the optimization which may change the outcome of the optimization. In order to represent the load at the output, a spring is attached to the output node in y direction which has a spring constant of 1N/mm. Input for this optimization will be used as the output of the first lever design which is 0.34mm in $-y$ direction (see Figure 11). This input is given from the input node shown in Figure 13. Topology optimization objective is defined as the maximization of output displacement in positive y direction. As volume constraint, decreasing volume of the design domain to %60 is also chosen as in the case of first lever design optimization run.

In Figure 14, results of topology optimization run can be seen. For this optimization, TOSCA gives an output node displacement of 0.8 mm (in y-direction). When the remaining elements from the topology optimization (all elements with non-zero density factor) are exported to ANSYS and same input is applied to the model with same boundary conditions, this analysis gives an output nodal displacement of 0.76mm (Figure 15). There is a reduction in amplification ratio of the final design for the second lever compared to the topology optimization results. This is due to the fact that in the physical model elements with density factors smaller than unity will have to be taken as unity. This results in a stiffer design thus decreasing the amplification ratio.

When the physical designs for the two levers are combined in series (as originally planned), it is theoretically expected that the output node displacement should be around 0.76mm for an input displacement of 0.05mm. That is, expected amplification ratio is

around 15 to 1. Afterwards, combined lever design is given in Figure 16. Displacement distributions can be seen in

Figure 17. It can be seen that the output node displacement is 0.207mm in +y direction. Output displacement was expected to be 0.76mm in positive y direction based on the optimized levers performance separately. Difference may be due to the fact the resistance coming from the spring attached to the second lever output node was not taken into account when optimizing the first lever. Effect of the spring resistance when optimizing the first lever mechanism can only be taken into account by an iterative process which may require multiple topology optimization runs. Instead, it probably makes more sense to try to optimize the geometry for both levers simultaneously by defining a design space that includes both levers. This is done in the second design iteration which is presented in the following section.

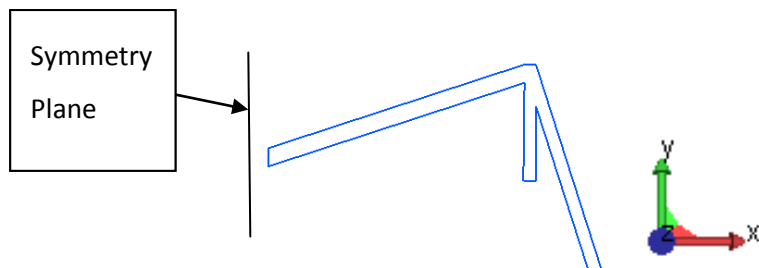


Figure 12 Conceptual design of the 2nd lever

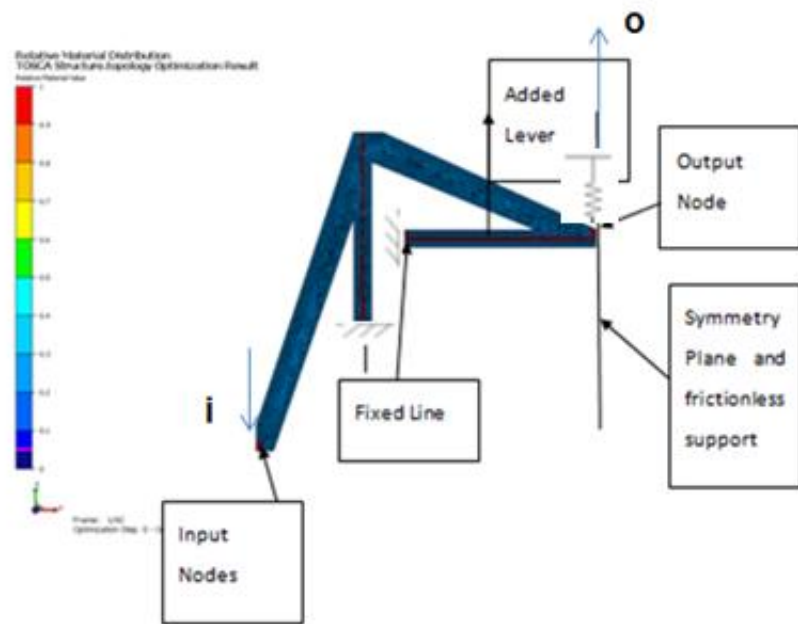


Figure 13 Finite element model of the design domain to be used in the topology optimization of the 2nd lever (added lever is for increasing the lateral stiffness of the mechanism)

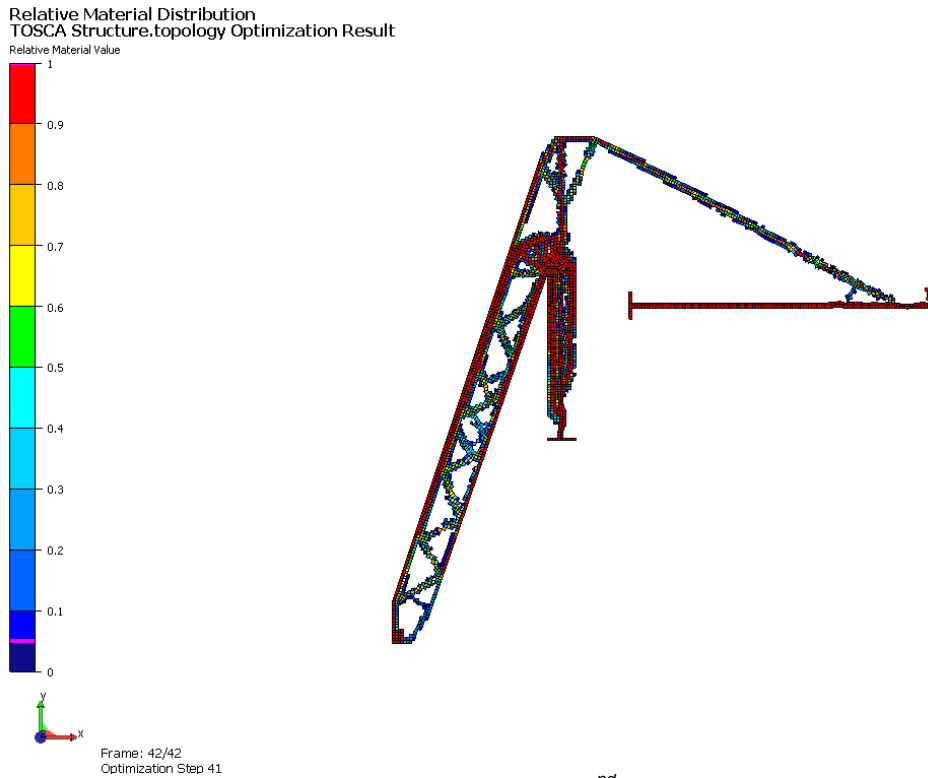


Figure 14 Result of the topology optimization for the 2nd lever (density factor distribution of all elements)

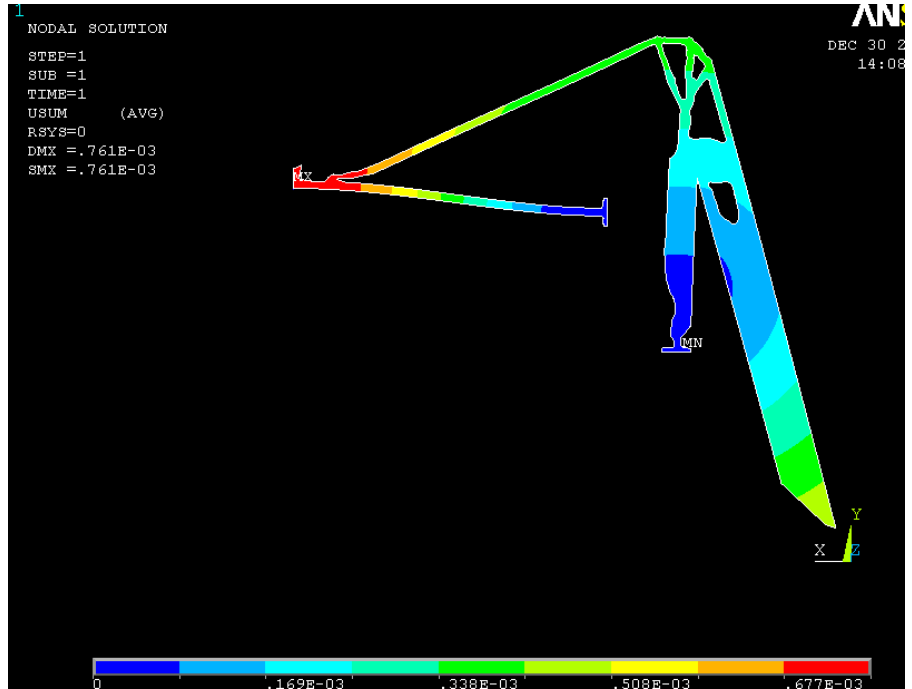


Figure 15 Static displacement analysis results for the final design of the 2nd lever

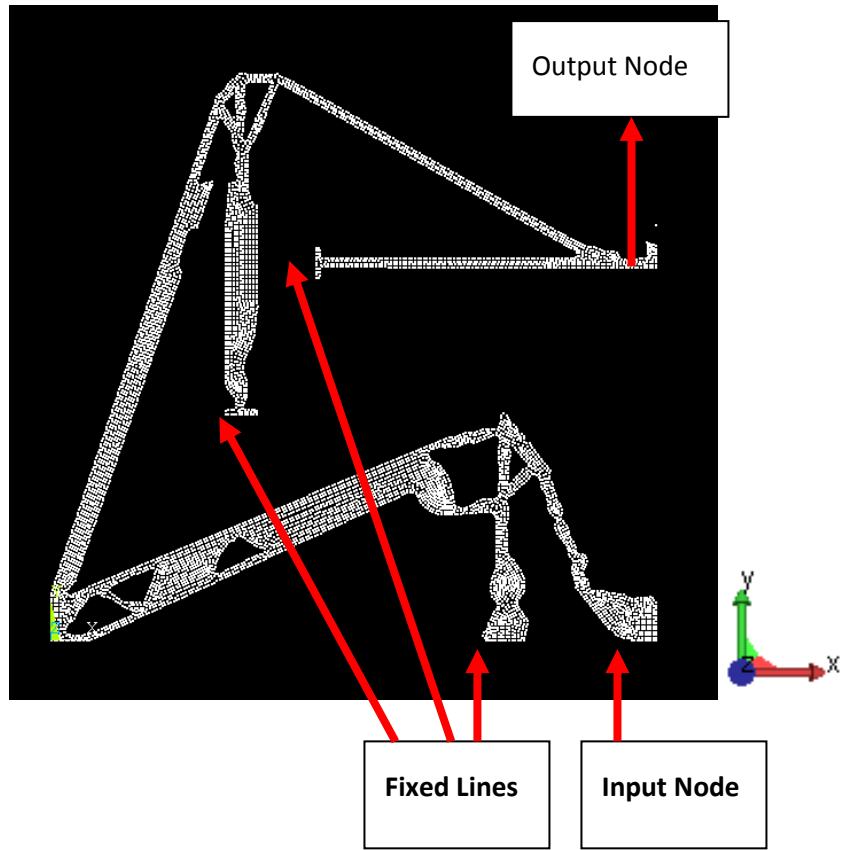


Figure 16 Finite element model of the compliant mechanism which is a combination of 1st and 2nd lever designs

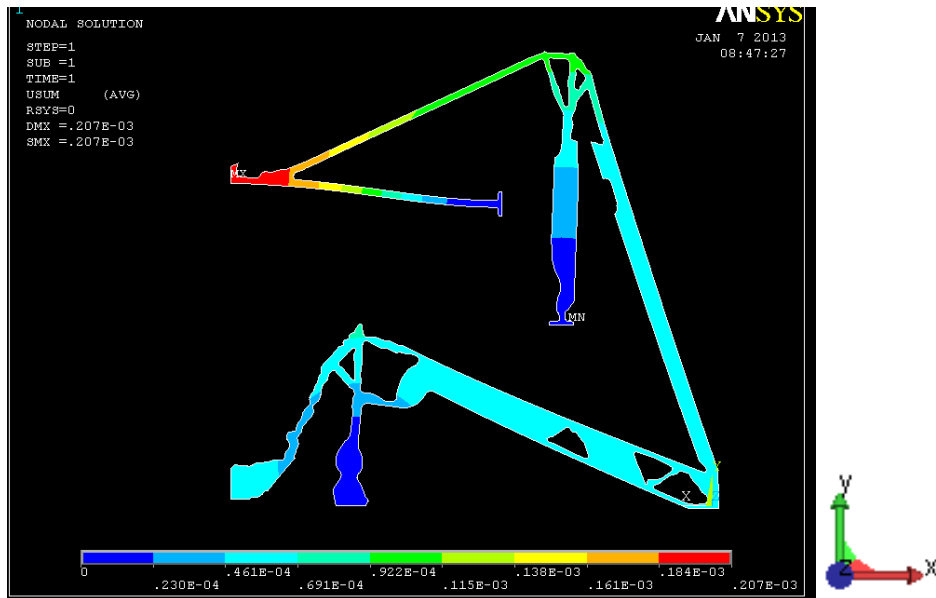


Figure 17 Static displacement analysis results of analysis done for the final design of the compliant mechanism

4.2.2 Second Design Iteration

In the second design iteration, first and second levers are optimized together.. Design domain occupies a square area of 80mmx80mm while not all the space within this domain is defined as part of the initial design domain. As seen in Figure 18, design domain represents the general geometry of the original double lever conceptual design. Design domain is actually similar to the design domains used for 1st and 2nd lever designs except some small changes such as increasing thicknesses of the lever arms and decreasing the thickness of the support lever. These changes are done with the experiences gained from the failed topology optimization process. The red elements are chosen as frozen elements which mean these elements will not diminish during optimization process and the green elements are design domain. Compliant mechanism that will be designed based on optimization results is expected to be of distributed compliant type mechanism, because almost all of the elements are included in design domain. In Figure 18 , green elements are part of the optimization elements and red elements are frozen elements which mean that they will be not eliminated during topology optimization. As displacement boundary conditions, three lines are fixed and input displacement is given from input line as 0.09 mm in positive y direction. Note that the piezostack actuator which will be used with the mechanism to be designed in this thesis has a maximum recommended maximum displacement of 0.09mm. In this optimization as in the case of the first design iteration, as the objective function, maximizing the output node in positive y direction is given.

A volume reduction ratio will also have to be defined in order to optimize the material distribution in the given design space. Volume reduction constraint is also an important factor that affects the results of the topology optimization runs thus various volume reduction constraints will have to be tried to obtain the best material distribution. Material used in this process is aluminum and thickness of the material is chosen as 2 mm. Resisting spring constant at the output node is taken as 3N/mm. Note that from some preliminary trial topology optimization runs, it has been observed that when no resisting spring is integrated to the model, density factor distribution for the same design space for a specific volume reduction constraint is independent of the material properties. That is if the output node has no constraints, topology optimization for a specific volume constraint and objective function combination gives the same distribution for any material.

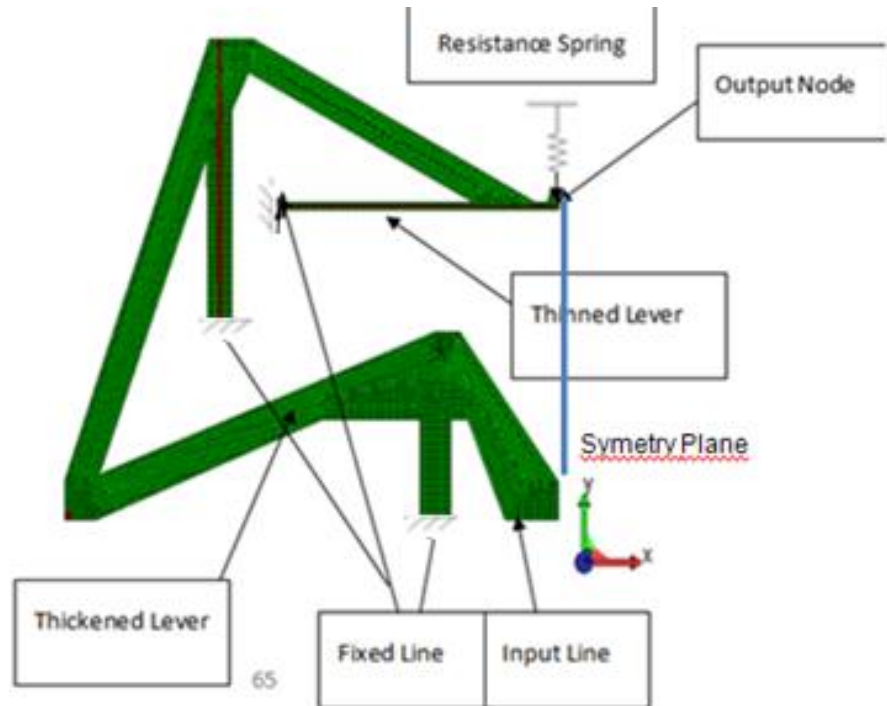


Figure 18 Finite element model of the design domain to be used in the topology optimization of the double lever mechanism: Second design iteration

As mentioned before various volume reduction constraint values will have to be tried to reach the best design configuration. Another analysis variable that significantly affects optimization results is the spring constant of the resistive spring attached to the output node. Volume reduction constraints of %40, % 60 and %80 are tried. Topology optimization runs are performed also for spring constants of $k=3\text{N/mm}$, $k=1\text{N/mm}$. It is observed that for certain combinations of volume reduction and resisting spring value does not give reasonable results like such as very low density factor elements that connects different regions of the remaining design space or very thin regions which are not manufacturable. Results for the combinations for which remaining design space looks feasible are presented in the thesis

In the first set of optimization runs, spring constant is first chosen as $k=3\text{N/mm}$ and then the volume constraints of 40%, 60%, and 80% are used in the optimization runs. Results will be investigated with respect to volume reduction constraint to see the effect of volume reduction constraint on amplification ratio of the mechanism.

In Figure 19 topology optimization results (density factor distribution) is given for the case of volume reduction constraint of %40(remaining design domain is expected to be 40% of the original design space defined in Figure 18). In Figure 20, output node y-displacement is given for the iterations performed during the topology optimization run. As can be seen from Figure 20, converged value for output node y-displacement is 1.15mm which corresponds to a mechanical amplification ratio of 13.

In Figure 21, topology optimization results (density factor distribution) is given for the case of volume reduction constraint of %60 (remaining design domain is expected to be 60% of the original design space defined in Figure 18). In Figure 22, output node y-displacement is given for the iterations performed during the topology optimization run. As can be seen from Figure 22, converged value for output node y-displacement is 1.22mm which corresponds to a mechanical amplification ratio of 13.5.

In Figure 23, topology optimization results (density factor distribution) is given for the case of volume reduction constraint of %80 (remaining design domain is expected to be

60% of the original design space defined in Figure 18). In Figure 24, output node y-displacement is given for the iterations performed during the topology optimization run. As can be seen from Figure 24, converged value for output node y-displacement is about 1.3mm which corresponds to a mechanical amplification ratio of 14.5.

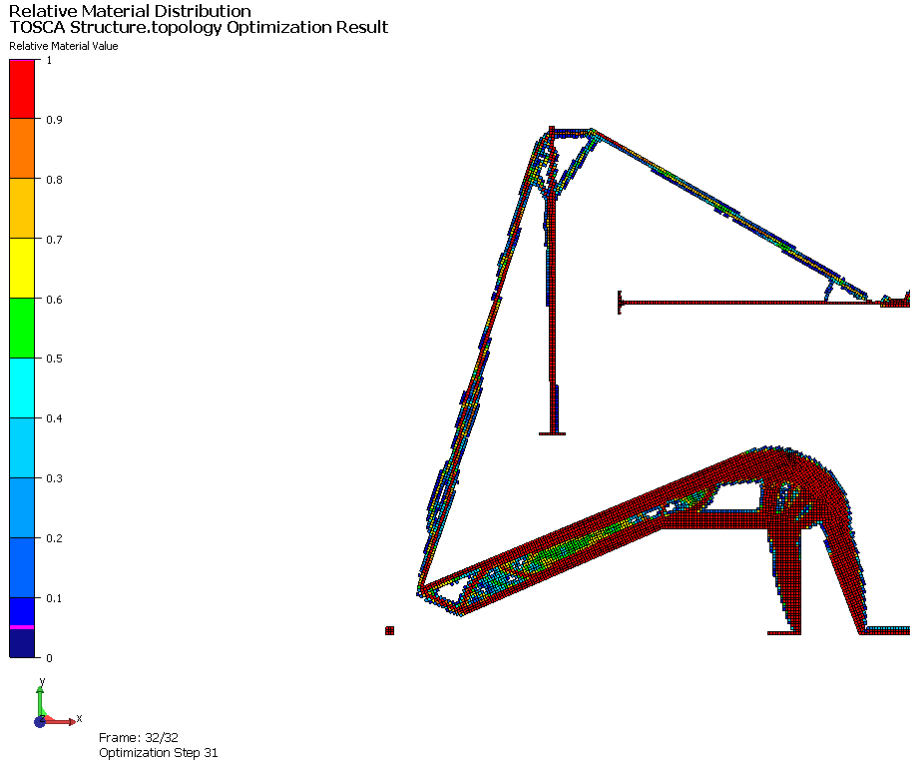


Figure 19 Result of topology optimization (density factor distribution) of the double lever design domain for a resistive spring constant of $k=3\text{N/mm}$ and volume reduction constraint of %40

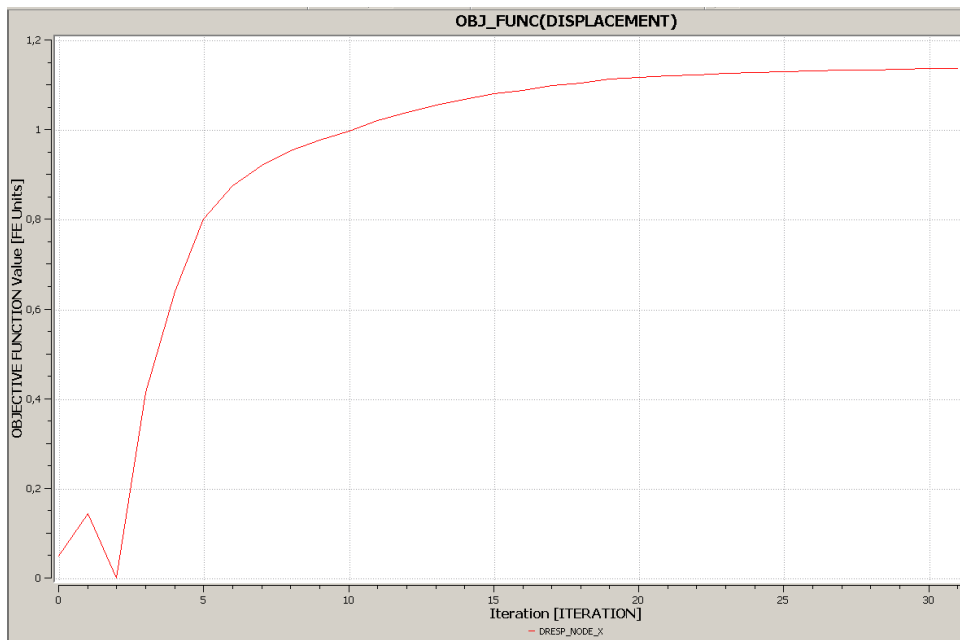


Figure 20 Output node y-displacement given as a function of iterations performed during the topology optimization run: for a resistive spring constant of $k=3N/mm$ and volume reduction constraint of %40

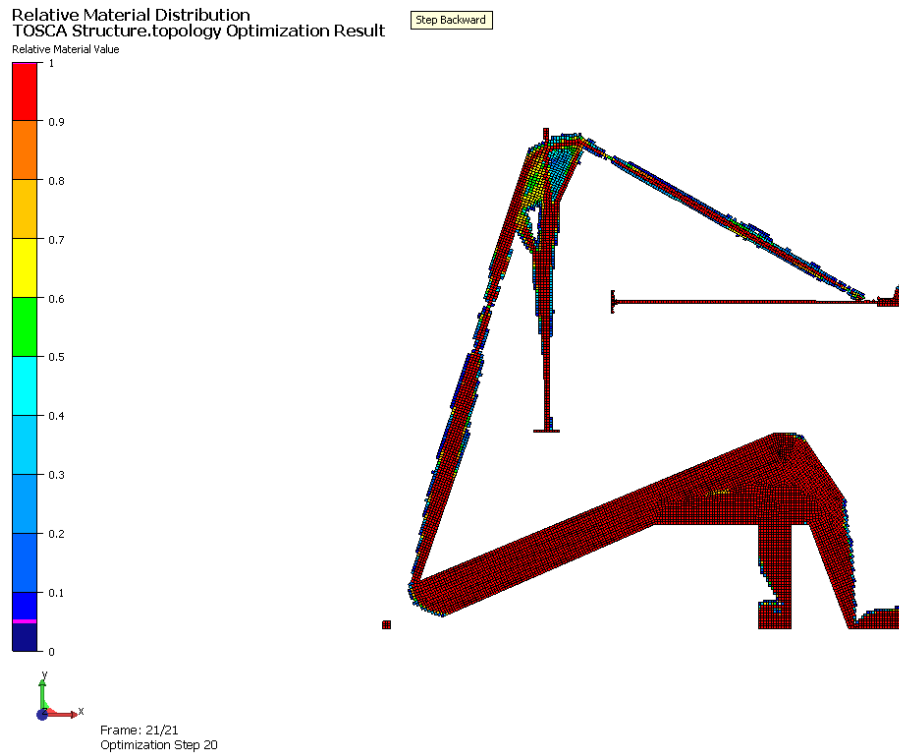


Figure 21 Result of topology optimization (density factor distribution) of the double lever design domain for a resistive spring constant of $k=3N/mm$ and volume reduction constraint of %60

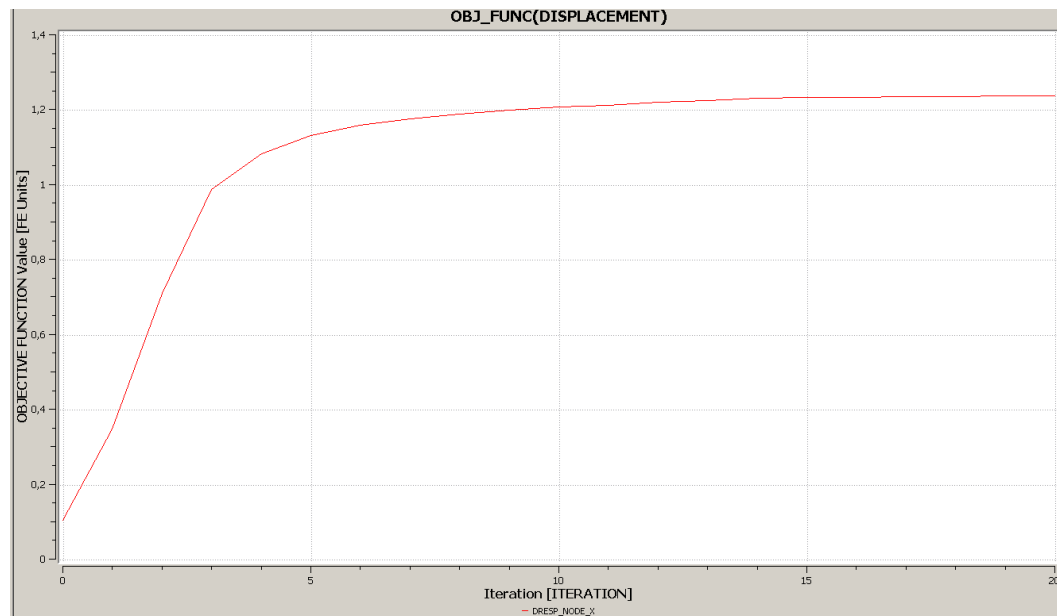


Figure 22 Output node y-displacement given as a function of iterations performed during the topology optimization run: for a resistive spring constant of $k=3N/mm$ and volume reduction constraint of %60

Relative Material Distribution
TOSCA Structure.topology Optimization Result

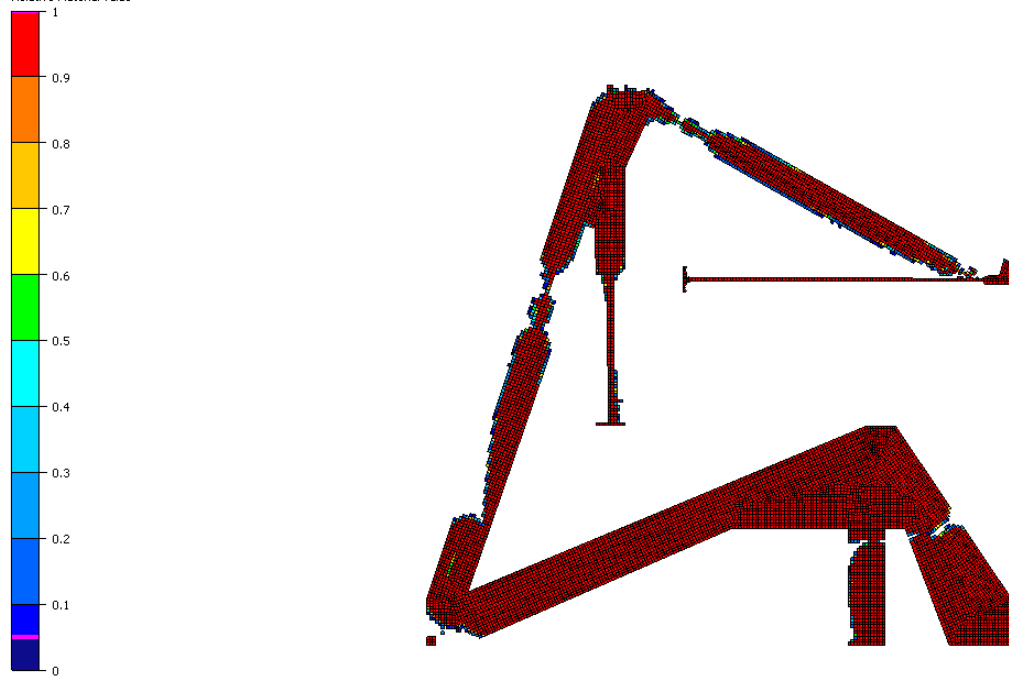


Figure 23 Result of topology optimization (density factor distribution) of the double lever design domain for a resistive spring constant of $k=3N/mm$ and volume reduction constraint of %80

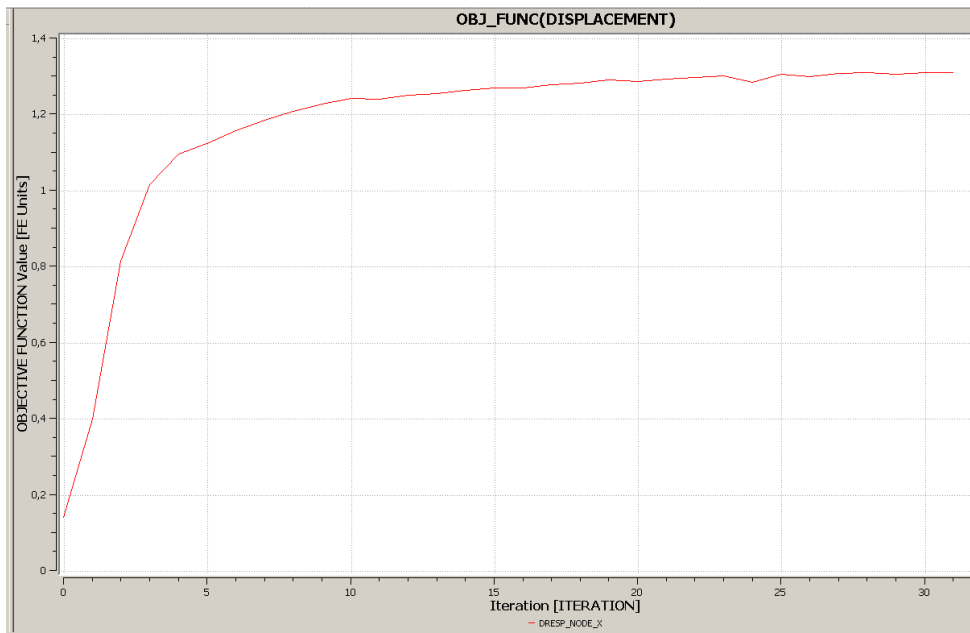


Figure 24 Output node y-displacement given as a function of iterations performed during the topology optimization run: for a resistive spring constant of $k=3N/mm$ and volume reduction constraint of %80

In the first set of optimization runs, spring constant is first chosen as $k=1\text{N/mm}$ and then the volume constraints of 40%, 60%, and 80% are used in the optimization runs. Results will be investigated with respect to volume reduction constraint to see the effect of volume reduction constraint on amplification ratio of the mechanism.

In Figure 25, topology optimization results (density factor distribution) is given for the case of volume reduction constraint of %40 (remaining design domain is expected to be 40% of the original design space defined in Figure 18). In Figure 26, output node y-displacement is given for the iterations performed during the topology optimization run. As can be seen from Figure 26, converged value for output node y-displacement is about 2mm which corresponds to a mechanical amplification ratio of 22.

In Figure 27, topology optimization results (density factor distribution) is given for the case of volume reduction constraint of %60 (remaining design domain is expected to be 60% of the original design space defined in Figure 18). In Figure 28, output node y-displacement is given for the iterations performed during the topology optimization run. As can be seen from Figure 28, converged value for output node y-displacement is about 2.1mm which corresponds to a mechanical amplification ratio of 23.

In Figure 29, topology optimization results (density factor distribution) is given for the case of volume reduction constraint of %80 (remaining design domain is expected to be 60% of the original design space defined in Figure 18). In Figure 30, output node y-displacement is given for the iterations performed during the topology optimization run. As can be seen from Figure 30, converged value for output node y-displacement is about 2.1mm which corresponds to a mechanical amplification ratio of 23.

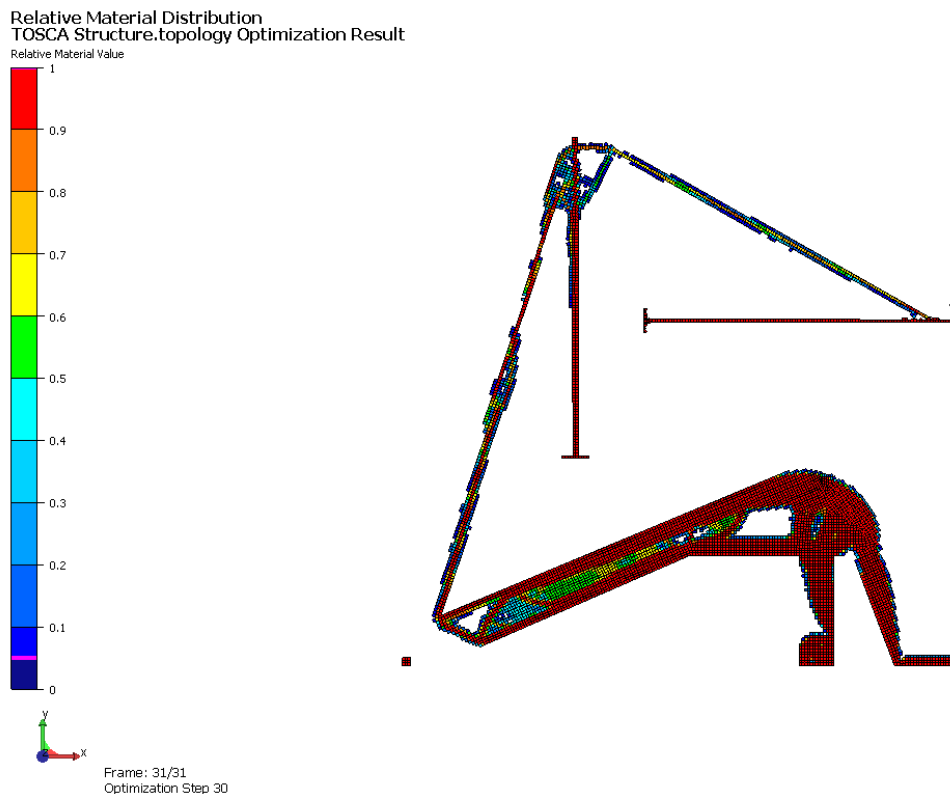


Figure 25 Result of topology optimization (density factor distribution) of the double lever design domain for a resistive spring constant of $k=1\text{N/mm}$ and volume reduction constraint of %40

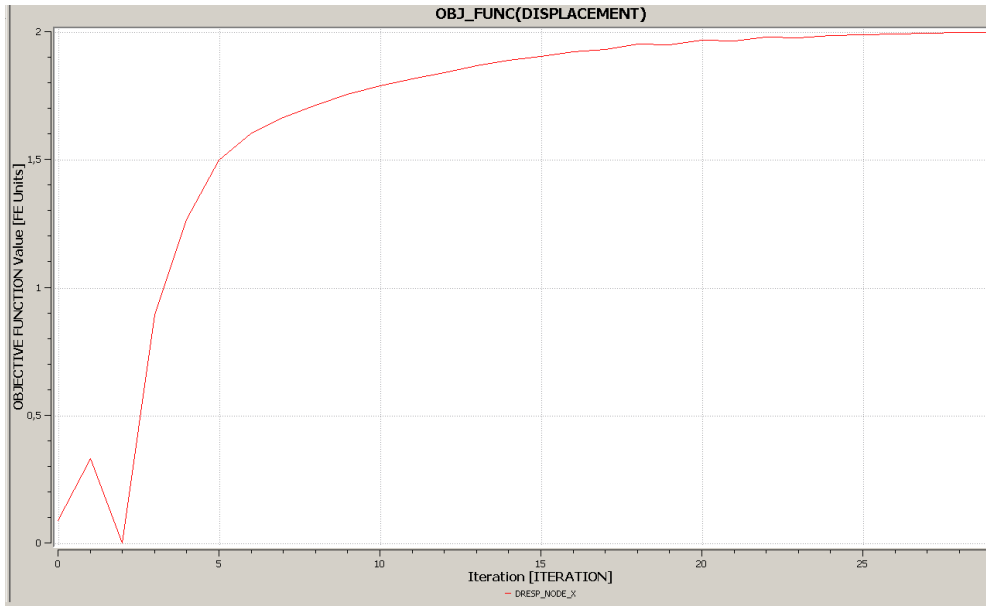


Figure 26 Output node *y*-displacement given as a function of iterations performed during the topology optimization run: for a resistive spring constant of $k=1\text{N/mm}$ and volume reduction constraint of %40

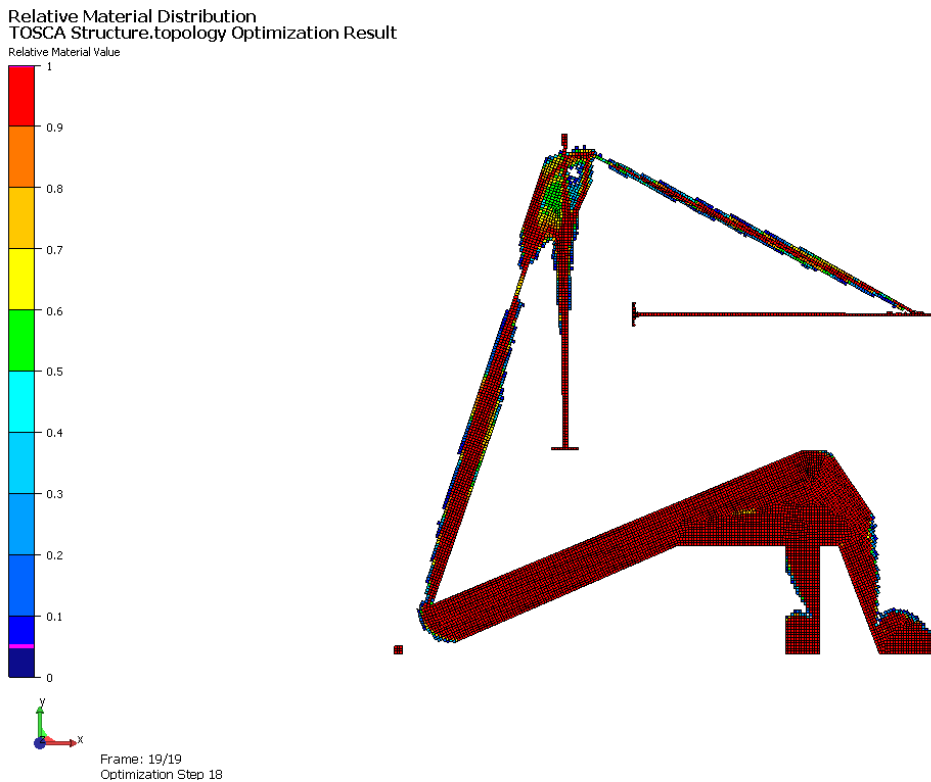


Figure 27 Result of topology optimization (density factor distribution) of the double lever design domain for a resistive spring constant of $k=1\text{N/mm}$ and volume reduction constraint of %60

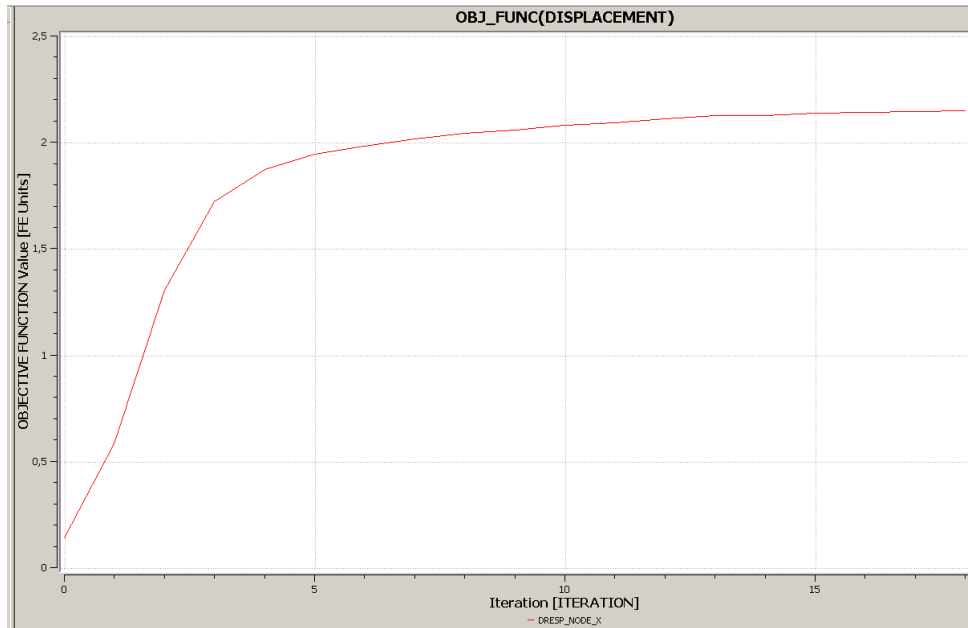


Figure 28 Output node y-displacement given as a function of iterations performed during the topology optimization run: for a resistive spring constant of $k=1\text{N/mm}$ and volume reduction constraint of %60

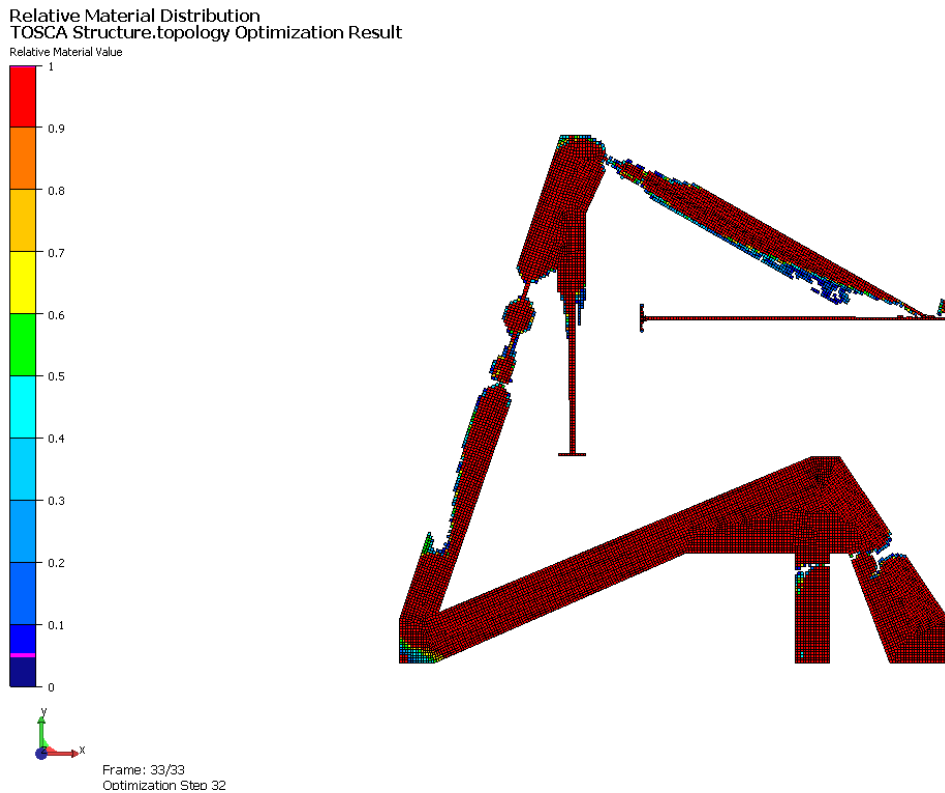


Figure 29 Result of topology optimization (density factor distribution) of the double lever design domain for a resistive spring constant of $k=1\text{N/mm}$ and volume reduction constraint of %80

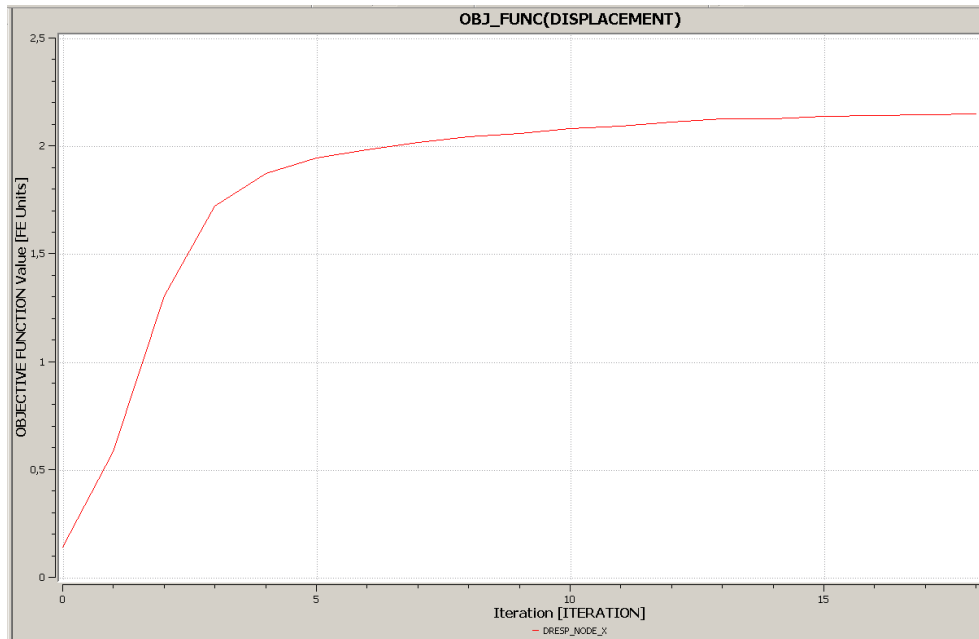


Figure 30 Output node y -displacement given as a function of iterations performed during the topology optimization run: for a resistive spring constant of $k=1\text{N/mm}$ and volume reduction constraint of %80

Considering the amplification ratios achieved for various optimization configuration and also the material density distributions, the configuration where $k=3\text{N/mm}$ and %60 volume reduction constraint is chosen as the best design for second design iteration. Results of the other configurations have too many low density elements especially near hinge areas and too many thin regions across the lever arms, which are not practically achievable.

As seen clearly from the Figure 22, output displacement is 1.2 mm for the selected design optimization. Using the density factor distribution obtained for the same configuration at the end of the topology optimization run (recall Figure 21), a final geometry is prepared in I-DEAS (see Figure 31) and this geometry is modeled in ANSYS using the same boundary and loading conditions used in topology optimization run.

As illustrated in Figure 32, output node y -displacement of the final geometry is 1mm which is about 18% smaller compared to the output displacement calculated in the last iteration of the topology optimization run (with spring constant 3N/mm and 60% volume reduction constraint). This difference is expected as discussed previously for the results of the first design iteration, since low density elements that exist in the topology optimization results (see Figure 27) and In CAD environment and ANSYS environment they cannot be modeled with their actual densities but their densities will have to be taken as unity. In Figure 33, results of the static displacement analysis done in ANSYS is shown but without any resistance spring at the output node. The output displacement is about 1.78mm which means the amplification ratio is almost 20. However this model is not a realistic model because there are two thin sections (see Figure 34) which has thicknesses of 0.2mm which cannot be produced. Thus these areas are modified and the thicknesses of these areas are increased.

Selected design domains were meshed with 0.4mm elements size and thin sections are evaluated according to this property. As mentioned before, the topology results with many low density elements are not close to analysis results. Thin section below 1 mm thin sections are cannot be produced easily to however with very carefully machining up to 0.6mm thin sections can be produced with wire erosion method. To sum up, by selection of presenting topology results, these logical reasons are considered.

In Figure 35, static displacement analysis of the modified compliant mechanism without any spring is illustrated. After thickening thin areas, output node y -displacement

decreases to 1.61 mm which means the amplification ratio decreases to 18 after modification. Afterwards, a full geometry with assembly details is created for this modified compliant mechanism as in Figure 36. Holes are created for screwing the compliant mechanism to the ground (i.e. to a fixing plate).

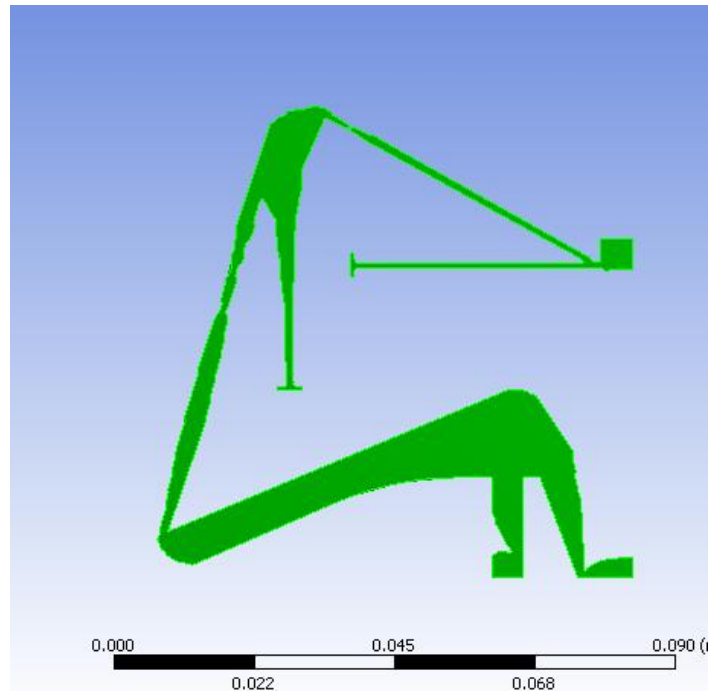


Figure 31 Final geometry of the double lever design obtained using the results of topology optimization (density factor distribution) of the original domain for a resistive spring constant of $k=3N/mm$ and volume reduction constraint of %60

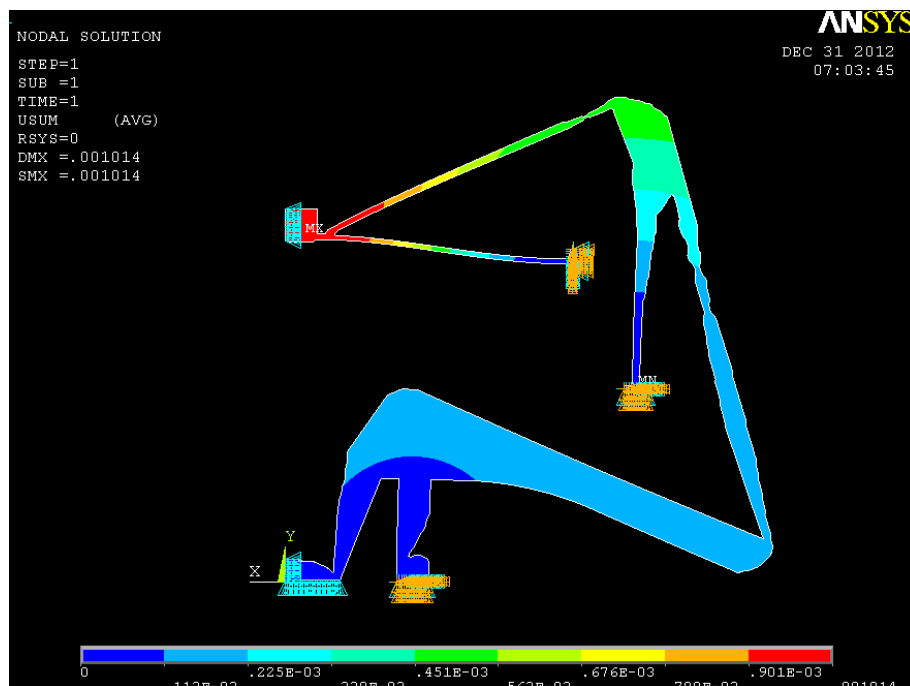


Figure 32 Displacement result of the second optimization, final design of the double lever mechanism without any resistance spring (Second design iteration)

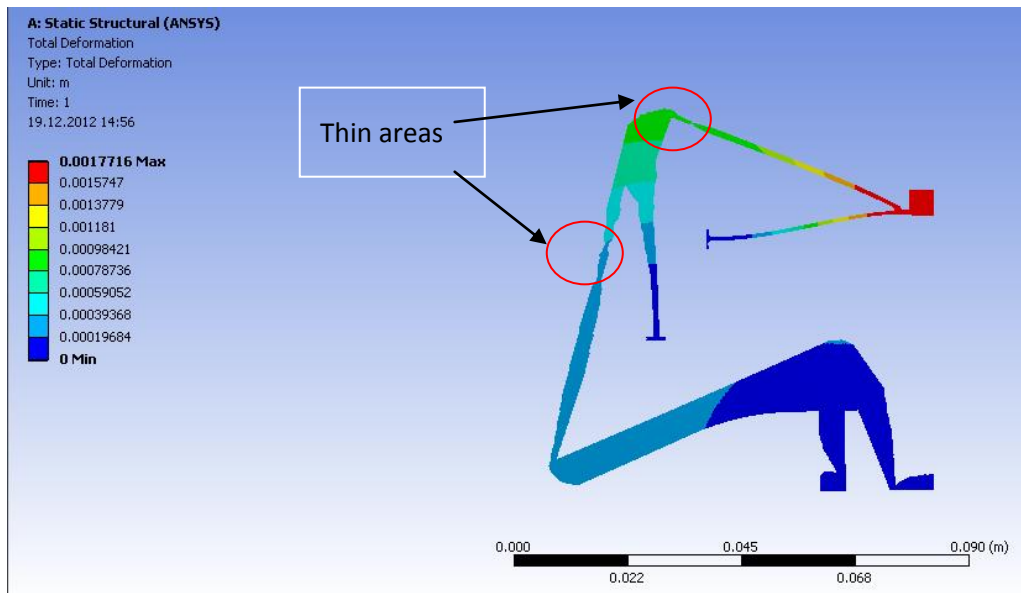


Figure 33 Displacement result of the final design of the double lever mechanism without any resistance spring (Second design iteration)

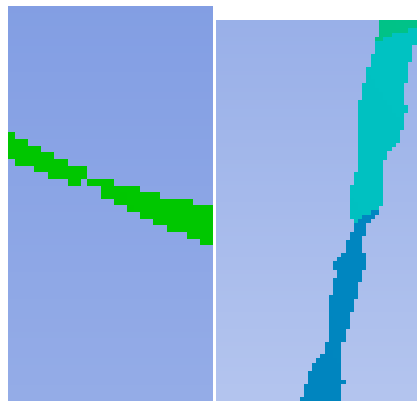


Figure 34 Thin areas of the final design of the double lever mechanism without any resistance spring (Second design iteration)

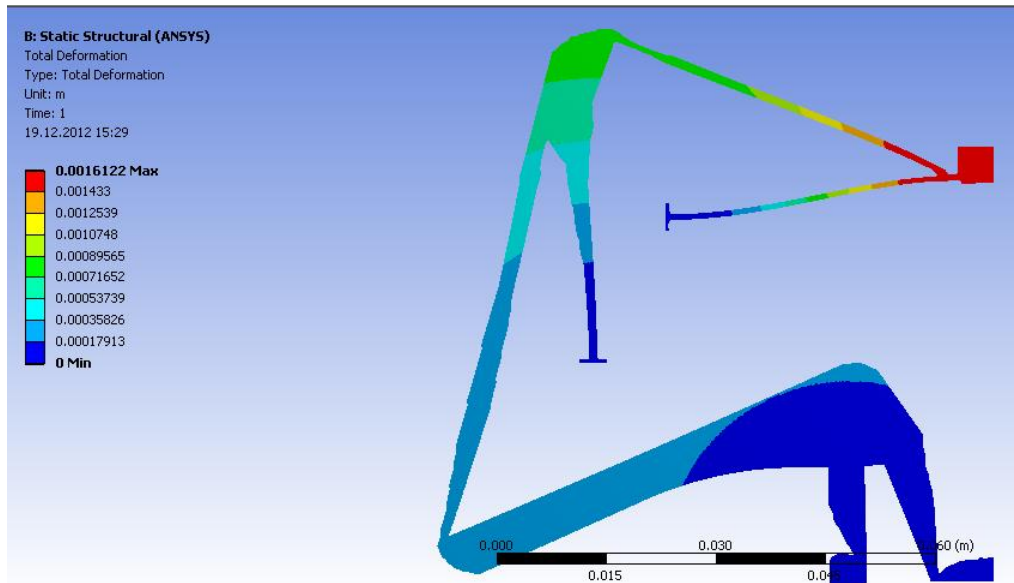


Figure 35 Displacement results of the modified final design (with thickened sections) of the double lever mechanism without any resistance spring (Second design iteration)

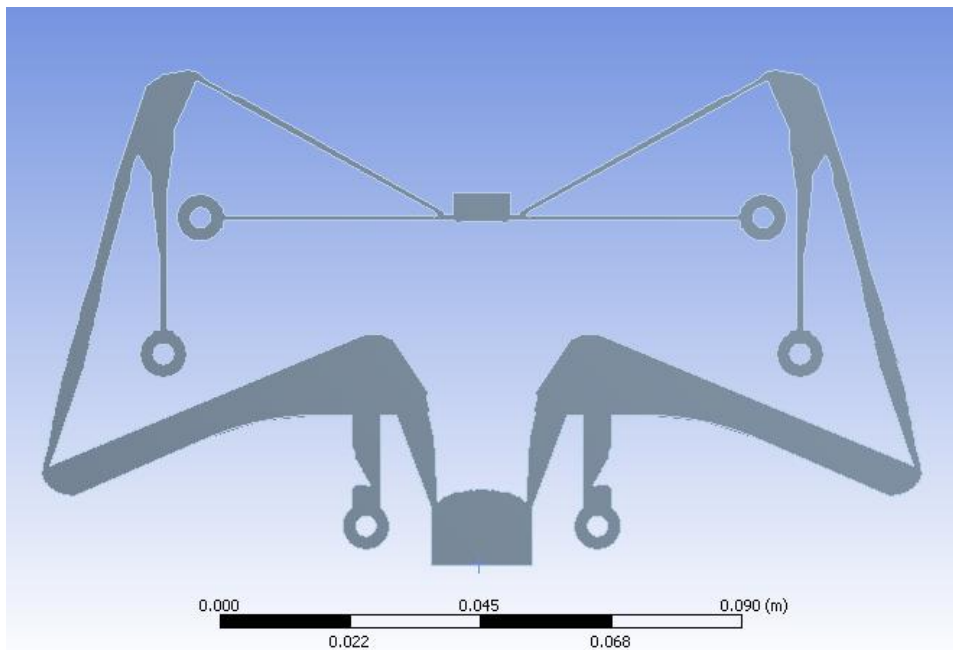


Figure 36 Full geometry of the modified final design (with thickened sections) of the double lever mechanism without any resistance spring (Second design iteration)

As mentioned before and shown in Figure 13, an additional hinge region was added to the output side of the second lever in the mechanism. This modification was made to increase the lowest natural frequency of the mechanism by increasing the lateral stiffness of the mechanism. However, this stiffening will also decrease overall mechanical amplification of the mechanism. In order to check this hypothesis mechanism is further modified by removing the hinge added to increase lateral stiffness (see Figure 37 for modified geometry). As seen in Figure 38, output node y-displacement for the modified

mechanism is about 1.97 mm which means that the mechanical amplification ratio increases from 18 to 22 after erasing the added stiffening hinge.

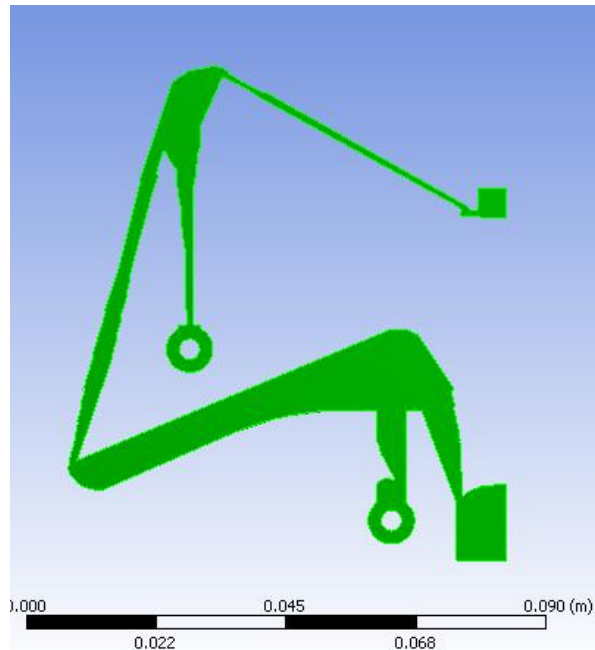


Figure 37 Full geometry of the second modified final design (with stiffening hinge removed) of the double lever mechanism without any resistance spring (Second design iteration): High amplification ratio version

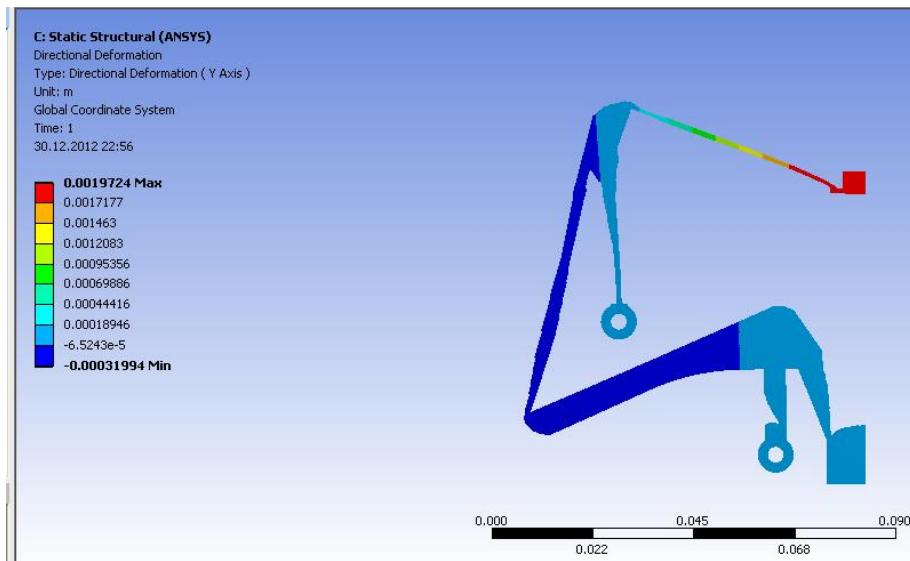


Figure 38 Displacement results of the second modified final design (with stiffening hinge removed) of the double lever mechanism without any resistance spring (Second design iteration): High amplification ratio version

4.2.3 Third Design Iteration

In previous design iterations, almost all parts of the design domain constitute the design space (i.e. very few frozen elements were defined). Resulting mechanisms were of distributed compliant type mechanisms. As a third design iteration, design space is defined such that material distribution around hinge areas for the two levers are included in the design domain but the main lever arms are included in frozen element set (see Figure 39). Such a design space definition is expected to give a lumped compliant mechanism.

For the third design iteration, material of the mechanism to be designed is selected as ABS Plus, the material used in a fast prototyping system available to us for manufacturing the designed mechanisms. This material has modulus of elasticity $E=2.36$ GPa however this material's poisson ratio is not defined. Its poisson's ratio is taken as 0.3. Density of the material is 1040 kg/m^3 . Yellow elements in the design domain are the design space elements in the design and the other elements are fixed (frozen elements). For this topology optimization resistive spring constant attached to the output node is taken as 0.2 N/mm . Spring amplitude is reduced compared to the second design iteration because the material used is about 30 times softer compared to aluminum used in the second design iteration.

In the optimization runs for third design iteration, spring constant is first chosen as $k=0.2 \text{ N/mm}$ and then the volume constraints of 70%, and 80% are used. Results will be investigated with respect to volume reduction constraint to see the effect of volume reduction constraint on amplification ratio of the mechanism.

In Figure 40, topology optimization results (density factor distribution) is given for the case of volume reduction constraint of %70 (remaining design domain is expected to be 70% of the original design space defined in Figure 39). In Figure 41, output node y-displacement is given for the iterations performed during the topology optimization run. As can be seen from Figure 41, converged value for output node y-displacement is about 0.7mm which corresponds to 8 amplification ratio.

In Figure 42, topology optimization results (density factor distribution) is given for the case of volume reduction constraint of %60 (remaining design domain is expected to be 60% of the original design space defined in Figure 39). In Figure 43, output node y-displacement is given for the iterations performed during the topology optimization run. As can be seen from Figure 43, converged value for output node y-displacement is about 0.7mm which corresponds to 8 amplification ratio.

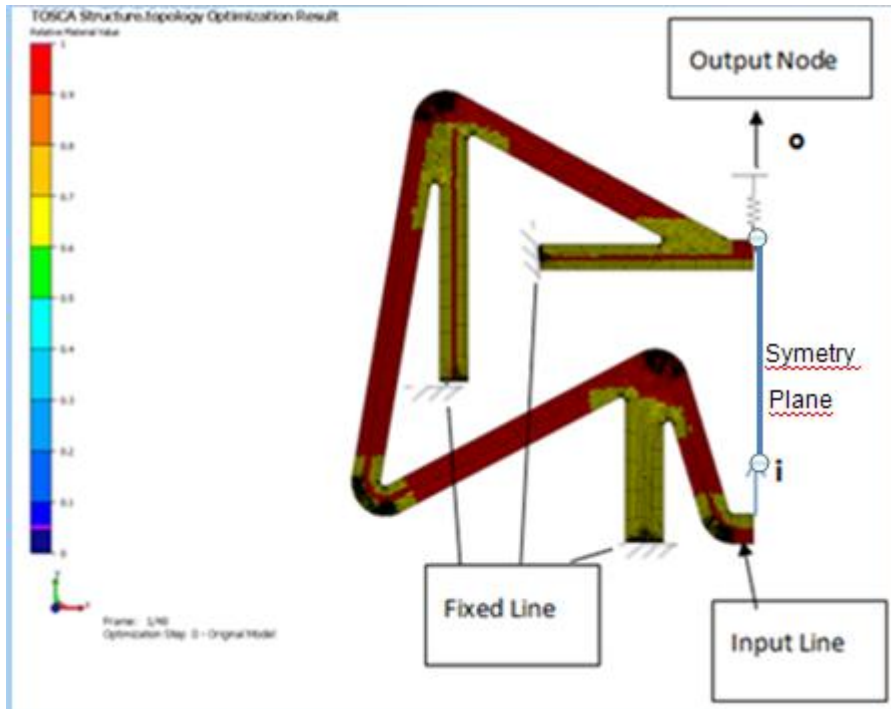


Figure 39 Finite element model of the design domain to be used in the topology optimization of the double lever mechanism: Third design iteration

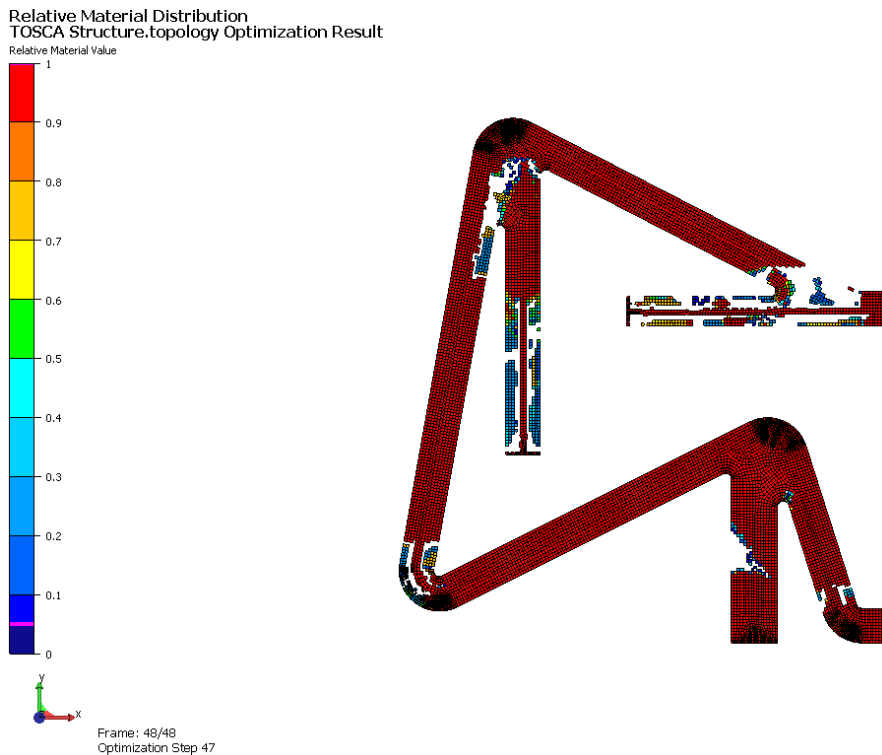


Figure 40 Result of topology optimization (density factor distribution) of the double lever design domain for a resistive spring constant of $k=0.2N/mm$ and volume reduction constraint of %70

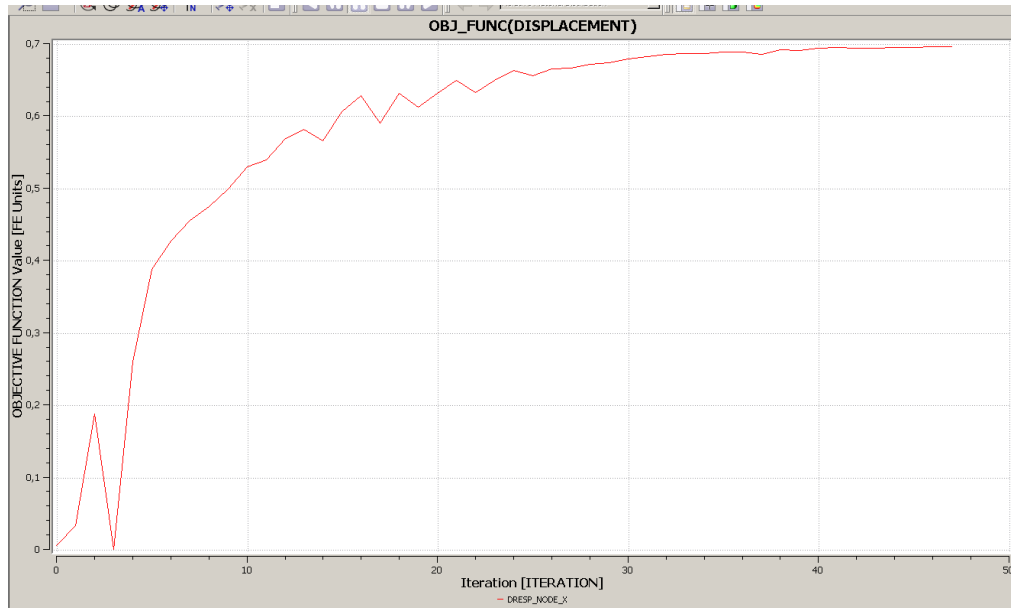


Figure 41 Output node y-displacement given as a function of iterations performed during the topology optimization run: for a resistive spring constant of $k=0.2N/mm$ and volume reduction constraint of %70

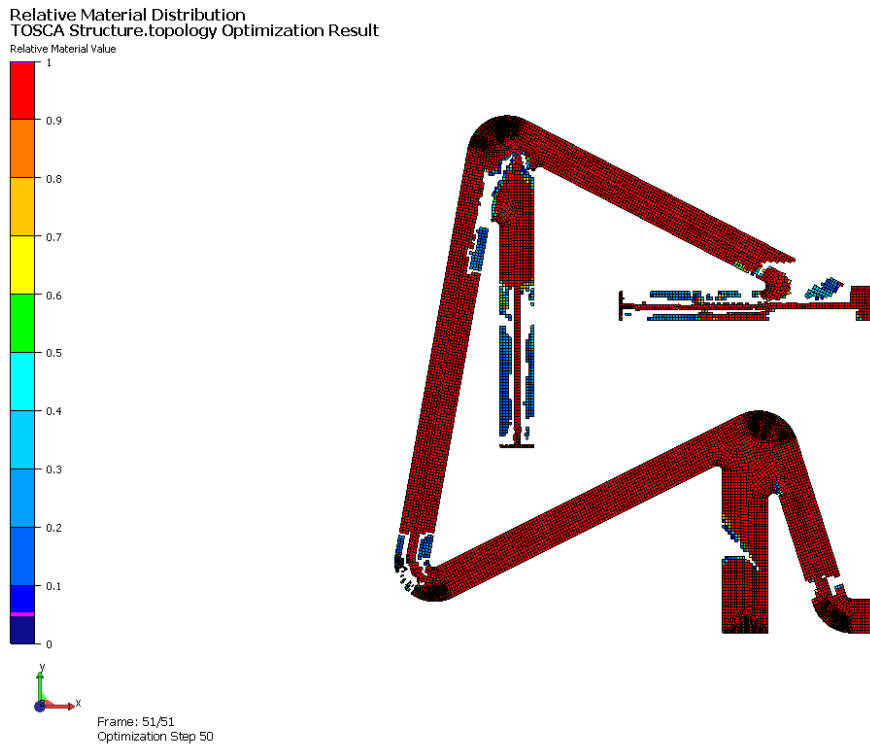


Figure 42 Result of topology optimization (density factor distribution) of the double lever design domain for a resistive spring constant of $k=0.2N/mm$ and volume reduction constraint of %80

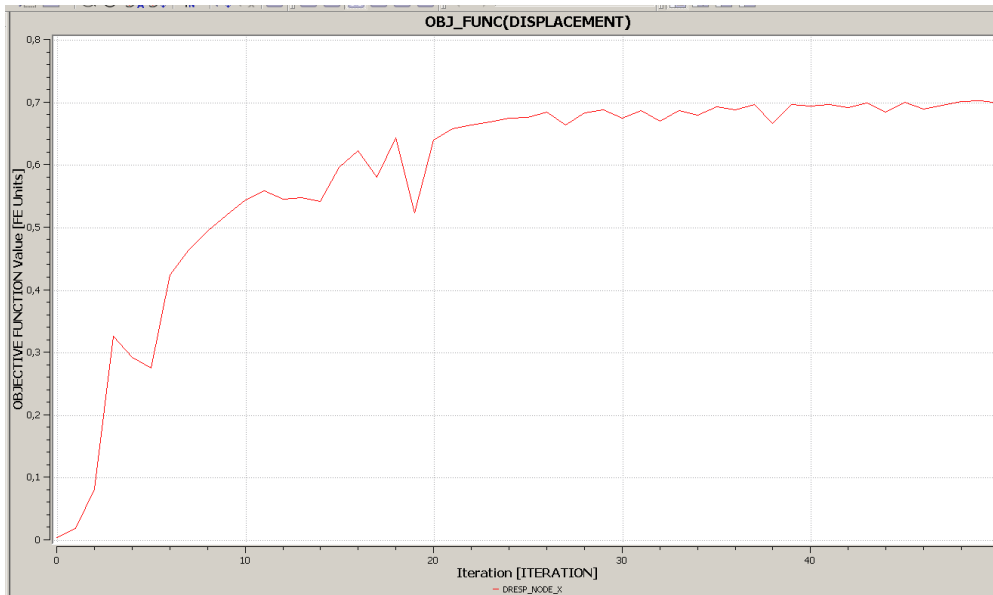


Figure 43 Output node y-displacement given as a function of iterations performed during the topology optimization run: for a resistive spring constant of $k=0.2\text{N/mm}$ and volume reduction constraint of %80

Many other topology optimizations are done with the design domain for the third design iteration by changing frozen elements. However none of them is selected due to impractical geometry results. One disadvantage of the results for the third design iteration is that around the hinge areas no element with unity density factor remains which is not physically realizable. Because of this, final modified design (see Figure 37), which has the highest amplification ratio will be manufactured and tested for design process verification purposes.

4.2.4 Detailed Analysis of the Selected Compliant Mechanism

In this section detailed analysis of the selected compliant mechanism will be done. Selected compliant mechanism is illustrated in Figure 37. Mechanism is analyzed in terms of its amplification ratio, input force, first natural frequency, and maximum stress condition to check for static failure.

To make the production easier in terms of time and cost, prototype mechanism will be produced using ULTEM 9085 which is a fast prototype machine material. This material has properties of $E=2,2$ GPa and ultimate tensile strength of the material is 71,6 MPa. Specific gravity of the material is 1,34 [17]. This material is selected because it has the highest ultimate tensile strength among other plastic fast prototype material options available to us. First of all the static analysis is done for finding the input force. According to these result, input force should be 16.3 N for half of the mechanism, which means that for the full geometry of the compliant mechanism 32.6 N force is required for creating a displacement input of 0.09mm when no resistive spring exists at the output. First natural frequency of this mechanism is 67Hz. From Figure 44, highest stress level in this mechanism can be seen to be 6,38 MPa which is less then ultimate tensile strength of ULTEM 9085 (72MPa)[17].

Finally, validity of using linear static analysis to design the mechanism is checked as shown in Table 5 where static displacement analysis results are compared for linear and nonlinear analysis options. As seen clearly from Table 5, mechanical amplification ratio is almost same with respect to input displacement for both analysis options. Thus compliant mechanism can be assumed to have a linear relationship between input and output displacements. In the next step, mechanism will have to be manufactured.

Table 5 Input and output displacements of the final design of the compliant mechanism for linear and nonlinear analysis options (no resistive spring is connected to the output node)

y-displacement at input node [mm]	y-displacement at output node [mm] (Linear analysis)	y-displacement at output node [mm] (Non-Linear analysis)	Mechanical Amplification Ratio (Linear)
0.03	0.657	0.662	22
0.06	1.315	1.332	22
0.09	1.973	2.010	22
0.12	2.631	2.693	22
0.15	3.288	3.383	22
0.2	4.384	4.54	22

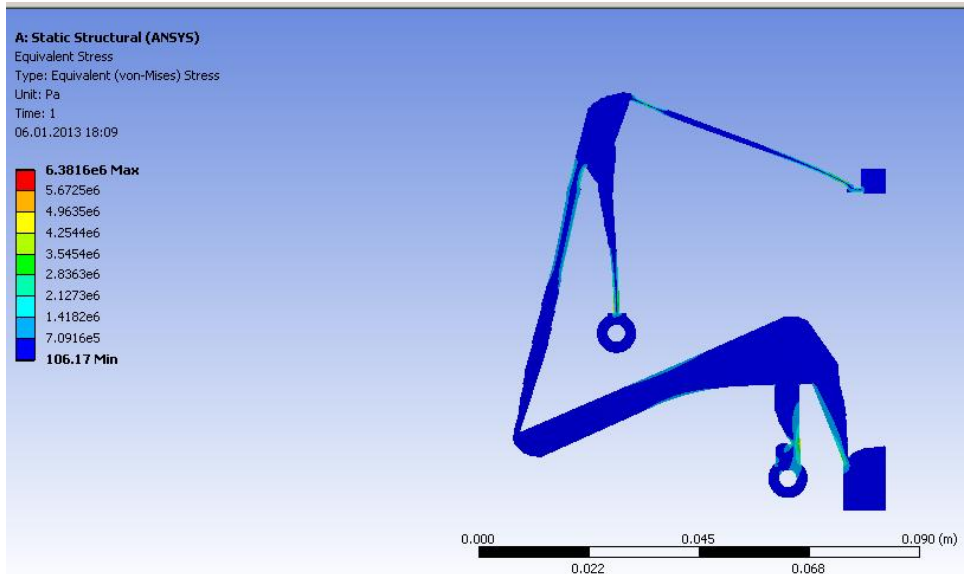


Figure 44 Stress results for selected compliant mechanism

As mentioned in this chapter, all of the analyses are done using static load case. In the user manual of TOSCA, it is mentioned that both static and dynamic optimizations can be done simultaneously. In this thesis, objective function is selected as maximizing the output displacement and the first natural frequency for the design domain, however this approach failed due to inconsistency between Tosca and ANSYS. The problem is investigated a lot even with the head office of TOSCA in Germany but they could not give any satisfying answer. After this effort, no more time is spent on this work and all the optimizations are performed for the static displacement based objective function.

CHAPTER 5

MANUFACTURING AND TESTING OF THE COMPLIANT MECHANISM

Selected compliant mechanism was illustrated in Figure 37. Prototype of this mechanism will be produced using a rapid prototyping machine from due to cheap cost and simple production process then production of mechanisms by wire erosion and milling from aluminum. Material used in the production is ULTEM 9085. Note that the design of the mechanism was done using aluminum while it is produced from another material. If no resistive spring is attached to the output node, the displacement characteristics of the mechanism should be same regardless of the material used since mechanism shows linear elastic behavior. Because this, tests are performed for no resistive spring case. Mechanism that is produced is given in Figure 45.

This mechanism is be integrated into a system which includes a base plate and two laser displacement sensors as shown in Figure 46. As seen clearly from Figure 46, two laser displacement sensors are used to measure the displacement at input and output ports of the compliant mechanism. Mechanism is modified at its boundary regions by adding through holes (see Figure 45) which can be used to fasten the mechanism to the base plate. Also another hole is drilled at the input port (see Figure 45) to be used for mounting the piezostack actuator. Another modification is to extend the mechanism in lateral direction at input and output locations so that small aluminum plates can be mounted on these extensions (see Figure 45 again). Laser displacement sensors can be used to measure the displacement of input and output ports of the mechanism by sending the laser beam to these extension plates added.

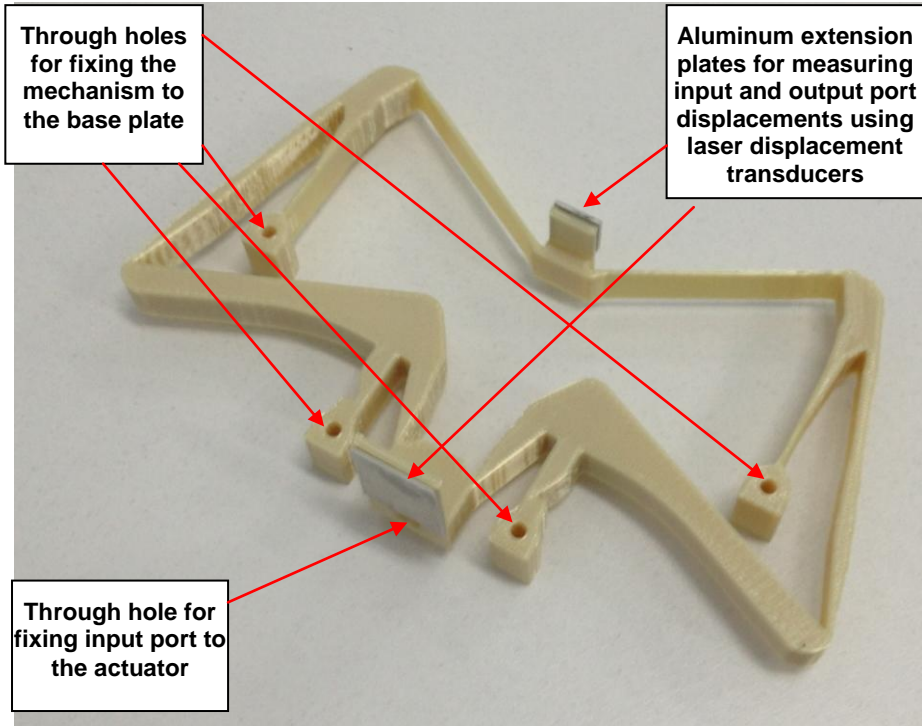


Figure 45 Prototype compliant mechanism manufactured using fast prototyping using ULTEM 9085 as fast prototyping material

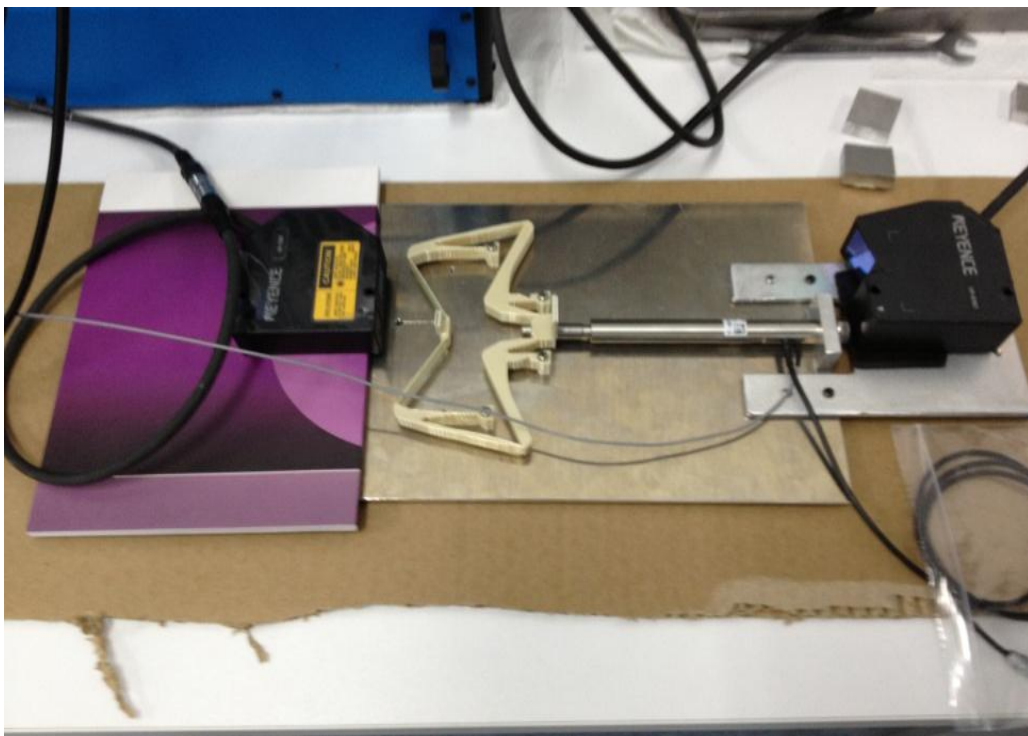


Figure 46 Piezostack actuator amplification system with base plate and sensors

Laser displacement sensors, which are going to measure input and output y-displacements are mounted on behind of the piezostack actuator and on the front of the output port of the compliant mechanism. With these sensors, displacements can be measured. One of the laser sensors has a displacement range of $\pm 4\text{cm}$ at a nominal distance of 15cm (Keyence LK-G157) and the other a displacement range of $\pm 0.5\text{cm}$ at a nominal distance of 3cm (Keyence LK-G37). After producing all of these parts and mechanisms, piezostack actuator is ready to give a displacement input. Whole setup for measuring static and dynamic performance of the prototype compliant mechanism is shown in Figure 47. A high voltage amplifier (see Figure 48) is used to amplify the control voltage used to drive the piezostack actuator. In Figure 48, digital display unit of the displacement sensors can also be seen. Another instrument used in this setup is an oscilloscope (see Figure 49) which was used monitor results of the displacement in terms of voltage output taken from the signal conditioning unit for the laser displacement sensors. Moreover a function generator (Figure 50) is used to produce the control voltage to drive the piezostack actuator. Last instrument used in the setup is a dynamic signal analyzer (Figure 51) which is used to measure the frequency response function of the compliant mechanism.

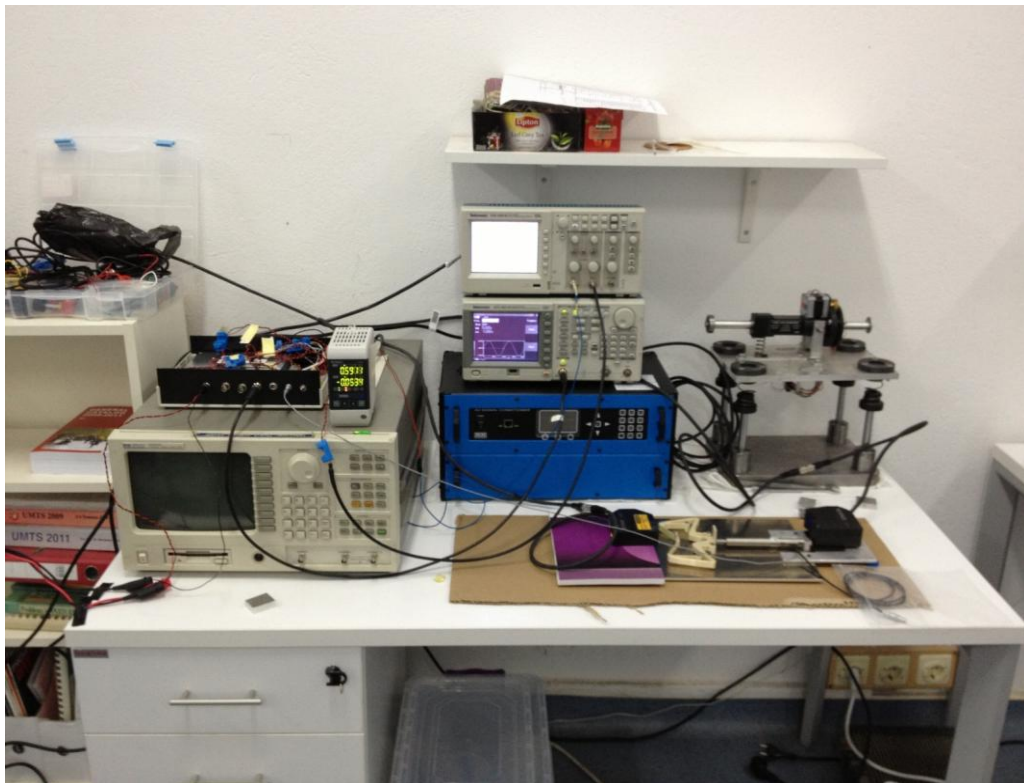


Figure 47 Setup for measuring static and dynamic performance of the prototype compliant mechanism

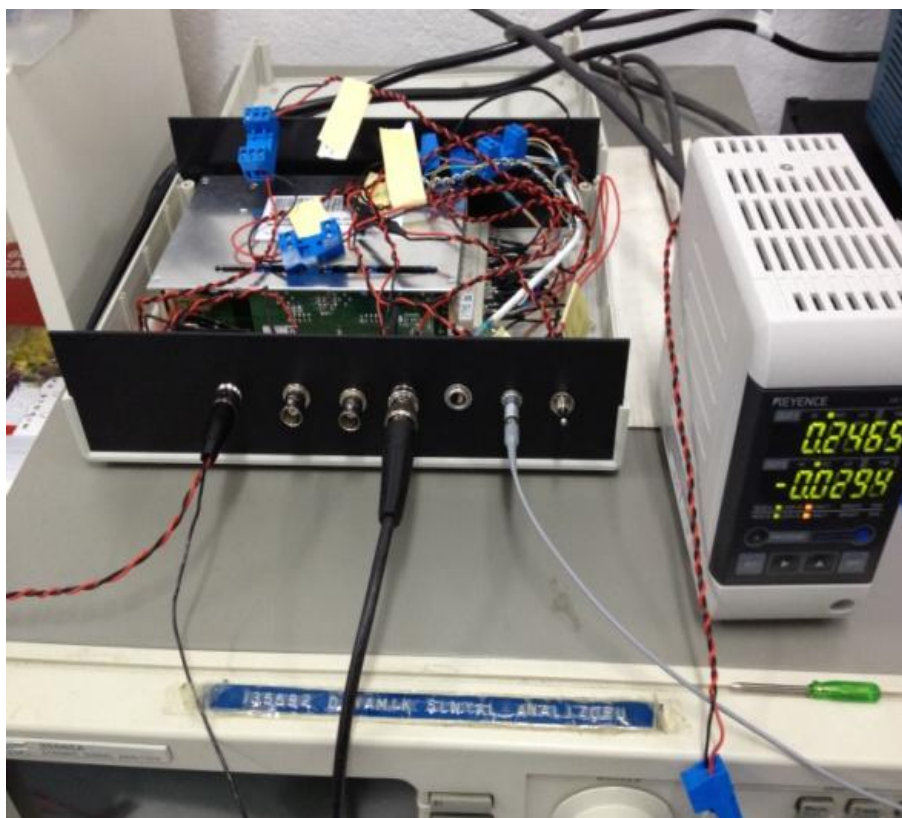


Figure 48 High voltage amplifier and display unit for laser displacement sensors

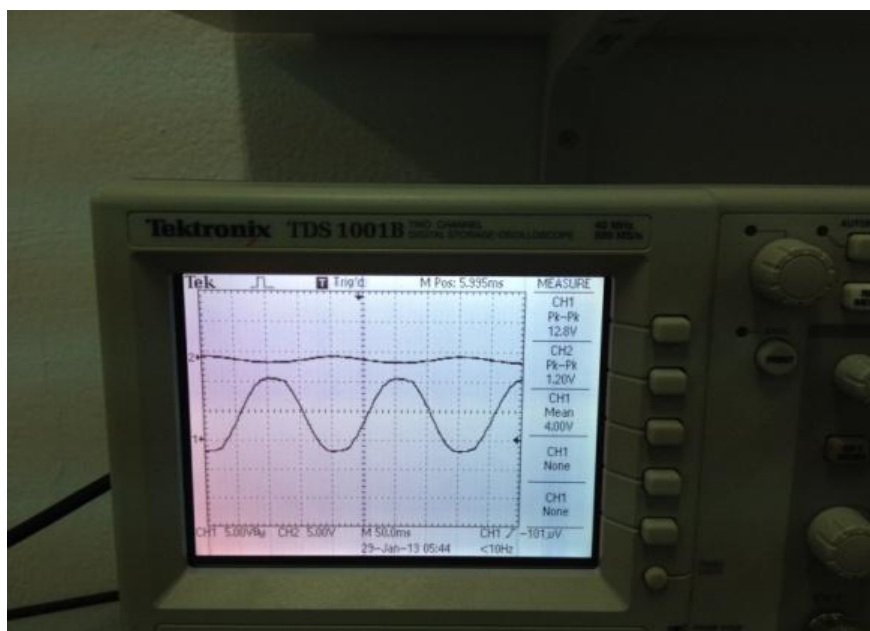


Figure 49 Oscilloscope

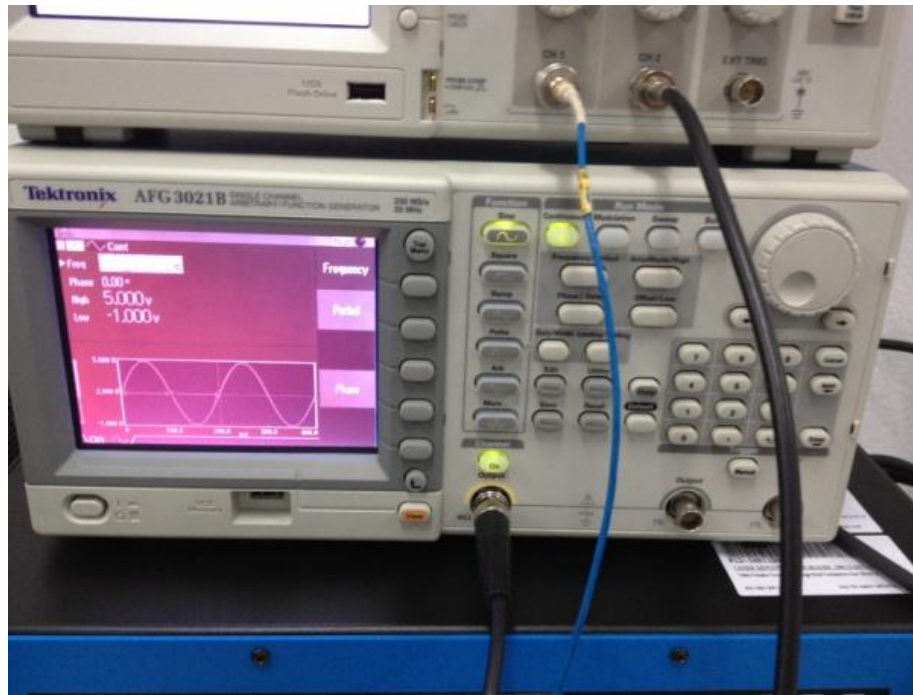


Figure 50 Function Generator

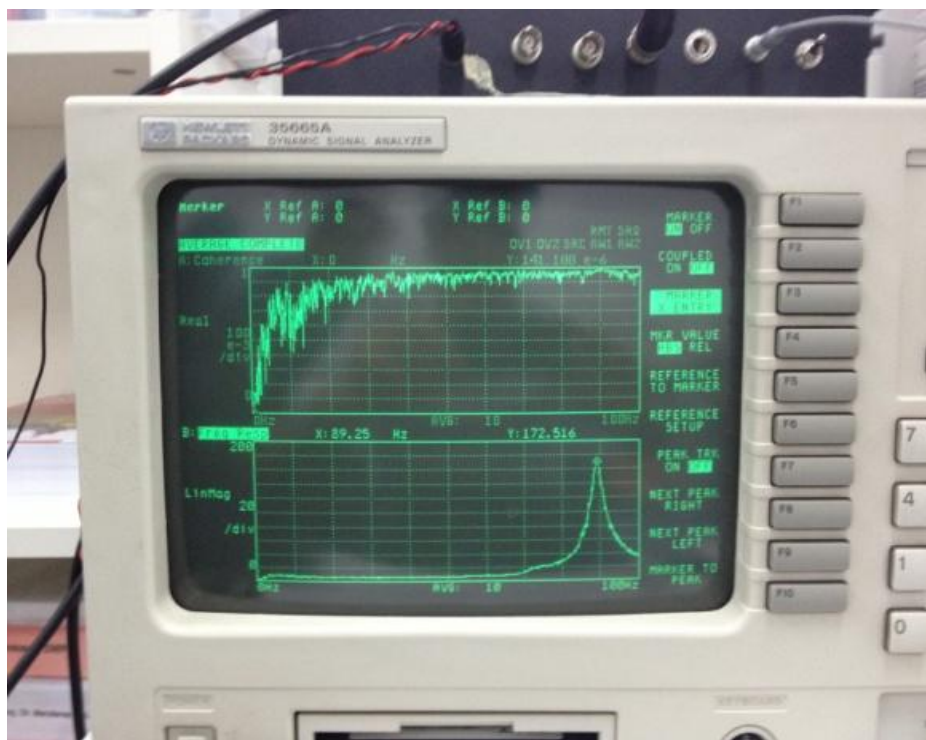


Figure 51 Dynamic signal analyzer

First static displacement measurements are taken as shown in Table 6. Various input displacements are applied and output displacements are measured. It is observed that mechanical amplification ratio changes with respect to input displacement which is

unexpected since mechanism is expected to behave linearly. Expected amplification ratio based on static linear displacement analysis of the mechanism with no resistive spring attached to the output node is 22. However, looking at the test results presented in Table 6 it is seen that a maximum ratio of 15 is obtained in actual experiments. This result is quite unexpected. Previous check of effect of nonlinear behavior (geometric nonlinearity) showed that mechanical amplification ratio was very little effected, i.e. 22 for linear case and for nonlinear case between 22,05 and 22,7 (see Table 5). So difference between experiments and analysis is not from geometric nonlinearity. Another reason may be due to anisotropic material behavior since fast prototyping manufacturing technique cannot produce a material distribution that is homogeneous. In order to check the effect of possible anisotropic material behavior on the displacement characteristics of the mechanism, an orthotropic material model is defined in ANSYS and static analysis are repeated. Three analyses are done by perturbing nominal young modulus of the material in three directions as shown in Table 7. Highest young modulus of elasticity is assumed to be 2.2 GPa and in the other two direction they are assumed to be 1.8 GPa for three cases. For isotropic case the static displacement was 1.97 mm for 0.09 mm input. As seen from Table 7 the results are similar to isotropic case.

Table 6 Static measurement results of the compliant mechanism: Comparison of experimental and analysis results

INPUT in mm	OUTPUT in mm	AMPLIFICATION RATIO	OUTPUT in ANSYS in mm	AMPLIFICATION RATIO in ANSYS
0.03	0.31	10,3	0,657	22
0.08	1.1	13,6	1,75	22
0.09	1.35	15	1,97	22

Table 7 Static displacement analysis results when orthotropic material model is used

	Case 1	Case 2	Case 3
Young Modules in x direction in GPa	2.2	1.8	1.8
Young Modulus in y direction in GPa	1.8	1.8	2.2
Young Modulus in z direction in GPa	1.8	2.2	1.8
Output node y-displacement in mm	1.99	1.96	1.93

Moreover, first natural frequency of the compliant mechanism is estimated by measuring the frequency response function of the mechanism using input and output node displacements as input and output responses respectively. A random signal is used to apply input through the input port of the mechanism and the output displacement is measured. Processing the input and output measurements, frequency response can be calculated as seen in Figure 52. Frequency response that is measured shows that the mechanism has a natural frequency of 89 Hz for the boundary conditions imposed by the setup. Same frequency response can also be obtained by simulating the test in ANSYS environment. Results are given in Figure 53 where for the nominal Young's modulus value of E=2.2 GPa of ULTEM 9085, estimated frequency response functions shows a first natural frequency of 105 Hz. This value is larger than what is measured. If Young's modulus is decreased to 1.8 GPa, first natural frequency can be reduced to 90 Hz which

is closer to experimental results. An initial conclusion would be that the effective material modulus of the manufactured mechanism is smaller than the nominal modulus value of the material used.

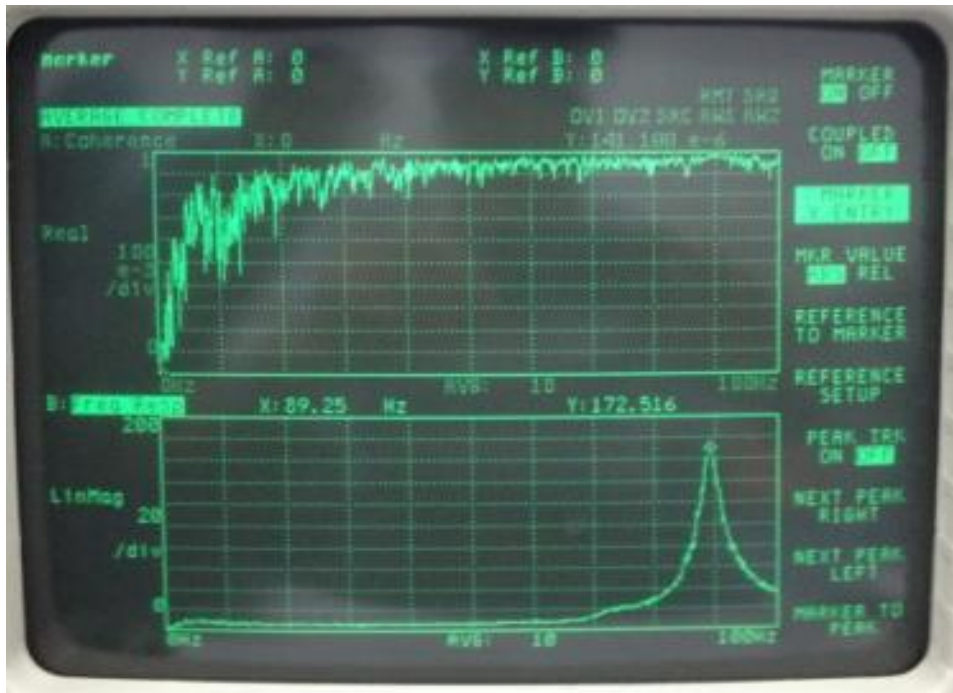


Figure 52 Frequency response function result on dynamic signal analyzer

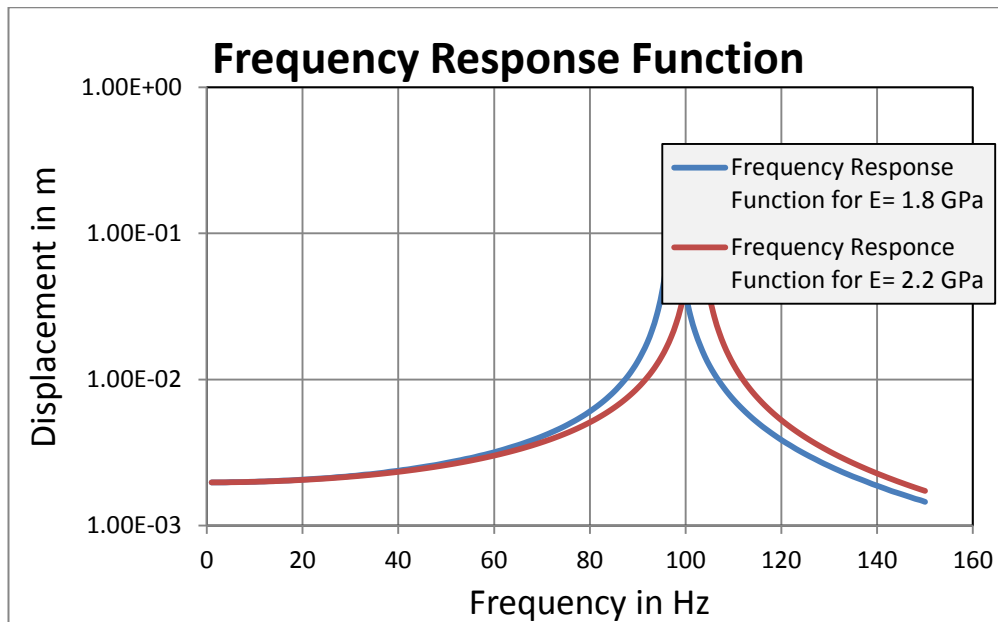


Figure 53 Frequency response function analysis result for different modulus of elasticity

In addition to these measurements, dynamic measurements are also taken for the compliant mechanism. During this measurement the input voltage is applied harmonically and the input frequency is change between 1 to 50Hz. Peak to peak amplitude of the

input is tried to be kept around 0.09 mm which is equal to the maximum stroke of the actuator used. Results for different frequencies are shown in Table 7. As seen clearly from Table 7, mechanical amplification ratio stays constant almost up to 25 Hz and after that at 50 Hz it is increased. This result is occurred due to getting close to the first natural frequency of the compliant mechanism (response is amplified due to resonance effect).

Table 8 *Dynamic measurement results of the compliant mechanism*

FREQUENCY Hz	INPUT Peak-to- peak amplitude in mm	OUTPUT peak-to- peak amplitude in mm	AMPLIFICATION RATIO
1	0.1	1.27	12.7
2	0.1	1.27	12.7
5	0.098	1.24	12.7
7,5	0.096	1.24	12.9
15	0.096	1.24	12.9
25	0.093	1.2	12.9
50	0.088	1.39	15.8

CHAPTER 6

CONCLUSION

In this thesis, a high frequency and high amplification ratio compliant mechanism is designed to be used to amplify the stroke of a piezostack actuator. Before designing the compliant mechanism many mechanisms are investigated in literature survey and using this literature survey conceptual designs are prepared. The main idea in conceptual design was lever mechanism and in this type of compliant mechanism mostly flexure hinges are used. These flexure hinges are optimized using parametric optimization of the hinge parameters (length, width, height etc). However, in this thesis the design of a double lever mechanism is selected and then designed using topology optimization method. Using topology optimization distributes the compliance throughout the mechanism rather than near hinge area, resulting in a distributed compliant mechanism.

In detailed design section, topology optimization runs are performed using different design domain, volume constraints, resistive spring constants and materials. During this detailed analysis section, it is found that by increasing the resistive spring constant, the amplification ratio is decreased. To solve this problem a new iteration is performed to have a compliant mechanism which has amplification ratio independent then resistive spring constant. However due to many low density elements in the solution of TOSCA, the results given from TOSCA and analysis results in ANSYS was inconsistent. Due to that reason no more effort is given to design such a compliant mechanism for this thesis study. However as a future work, a compliant mechanism which has a amplification ratio independent of resistive spring constant can be modeled by using piezoelectric patch actuator. By using them, the stiffness of the compliant mechanism near hinge areas can be controlled and adjusted according to the need of amplification ratio.

In the detailed design phase, topology optimization was originally intended to be used for both statically and dynamically optimize the geometry. However due to some software problems in TOSCA, static and dynamic objective functions could not be defined simultaneously. It has been asked to TOSCA staff, but no solution was offered. So topology optimization was performed for only static displacement objective functions (i.e. maximizing output node displacement for a given input node displacement). First natural frequency maximization was not included in the optimization run but it was calculated using the resulting material distribution that comes out of the topology optimization run for each iteration. After finishing the detailed design the mechanisms and the setup are manufactured. A setup is prepared such that it can be used test dynamic and static performances of the designed compliant mechanism.

Comparing test results and analysis results, it can be seen that the mechanical amplification ratio is expected to be 22 however it is found by testing about 13. This can be due to not clear material properties or tolerances in manufacturing. The tolerances in hinges should be very small however by fast prototype machining these tolerances cannot be achieved easily. Furthermore this mechanism can be produced from aluminum by using wire erosion to see the results by a fine machining and by an isotropic material. On the other hand lowest natural frequency of the manufactured mechanism turned out to relatively closer to the analysis results..

To conclude, the mechanism should be manufacturing by using an isotropic material like aluminum and high CNC or wire erosion technology in order to eliminate uncertainties in material properties which may improve correlation between analysis and test results. Due to high cost and high manufacturing time, during this thesis fast prototype

manufacturing technology is used. In further applications, with more budget more advanced manufacturing technologies can be used.

REFERENCES

- [1] K.B. Choi, J.J. Lee, S. Hata, "A piezo-driven compliant stage with double mechanical amplification mechanisms arranged in parallel", June 2010, *Sensors and Actuators A* 161 (2010) 173–181
- [2] R.F. Osborn, S. Kota and J.A. Hetrick "Active flow control using high frequency compliant structures" June 2004, *JOURNAL OF AIRCRAFT*, Vol. 41, No. 3, May–June 2004
- [3] M. Frecker and S. Canfield "Optimal design and experimental validation of compliant mechanism, Mechanical amplifiers for piezoceramic stack actuators" *JOURNAL OF INTELLIGENT MATERIAL SYSTEMS AND STRUCTURES*, Vol. 11—May 2000
- [4] H.W. Ma, S.M. Yao, L.Q. Wang, Z. Zhong "Analysis of the displacement amplification ratio of bridge type flexure hinge" May 2006, *Sensors and Actuators A* 132 (2006) 730–736
- [5] D.C. Handley, T.F. Lu, Y.K. Yong, W.J. Zhang "A simple and efficient dynamic modeling method for compliant micro positioning mechanisms with flexure hinges" *SPIE International Symposium on Microelectronics, MEMS, Nanotechnology Perth, Australia Dec 2003*
- [6] S. KOTA, J. JOO, Z. LI, S.M. RODGERS AND J. SNIEGOWSKI "Design of compliant mechanism- Application to MEMS" *Analog Integrated Circuits and Signal Processing*, 29, 7–15, 2001
- [7] L. Ren, R. Yang, W. Zhang "Topology optimization design for two-material micro compliant mechanism with stress constraint" 978-1-4244-9439-2/11©2011 IEEE
- [8] G.W. Jang, K. J. Kim, Y. Y. Kim "Integrated topology and shape optimization software for compliant MEMS mechanism design" *Advances in Engineering Software* 39 (2008) 1–14
- [9] S. Kota, J. Hetrick, Z. Li, and L. Saggere "Tailoring Unconventional Actuators Using Compliant Transmissions: Design Methods and Applications" *IEEE/ASME TRANSACTIONS ON MECHATRONICS*, VOL. 4, NO. 4, DECEMBER 1999
- [10] S.C. Huang, G.J. Lan "Design and Fabrication of Micro Compliant Amplifier with Topology Optimal Compliant" NSC 93-2212-E-151-007
- [11] www.cedrat.com, last access 1.1.2013
- [12] Stuart T. Smith "Flexure Elements of Elastic Mechanism (2000), Gordon And Breach, [13] Nicolae Lobontiu "Compliant Mechanisms ,Design of Flexure Hinges"(2003), Crc Press, New York
- [14] Larry H. Howell "Compliant Mechanisms"(2002) ,John Wiley And Sons Inc, New York
- [15] Luenberger D. G. , "Intorducton To Linear And Non-Linear Programming"(1984) ,Springer, Berlin
- [16] M.P. Bendsoe, O. Sigmund "Topology Optimization Theory Methods and Applications"(2003), Springer, Berlin
- [17] www.mayweb.com, last access 12.12.2012